Nano Today (2011) 6, 91—109

available at www.sciencedirect.com

ScienceDirect

journal homepage: www.elsevier.com/locate/nanotoday

REVIEW

Nanostructured photoelectrodes for dye-sensitized solar cells

Qifeng Zhang, Guozhong Cao*

Department of Materials Science and Engineering, University of Washington, Seattle, WA 98195, United States

Received 16 October 2010; received in revised form 21 December 2010; accepted 23 December 2010
Available online 21 January 2011

KEYWORDS
Dye-sensitized solar cell;
Nanostructure;
Nanoparticles;
Nanowires;
Aggregates;
Light scattering

Summary Nanotechnology opens a door to tailing materials and creating various nanostructures for use in dye-sensitized solar cells. This review classifies the nanostructures into (1) nanoparticles, which offer large surface area to photoelectrode film for dye-adsorption, (2) core—shell structures, which are derived from the nanoparticles however with a consideration to reduce charge recombination by forming a coating layer, (3) one-dimensional nanostructures such as nanowires and nanotubes, which provide direct pathways for electron transport much faster than in the nanoparticle films, and (4) three-dimensional nanostructures such as nanotetrapods, branched nanowires or nanotubes, and oxide aggregates, which not only emphasize providing large surface area but also aim at attaining more effective light harvesting and charge transport or collection. The review ends with an outlook proposing that the oxide aggregates are a potentially promising structure which may possibly achieve higher efficiency than the record by reason that the bifunction of aggregates in providing large surface area and generating light scattering allows for photoelectrode film thinner than usual and thus decreases the charge recombination of DSCs.

Introduction

Nanoscience and technology is a subject studying the materials with the dimensions ranging from several nanometers to several hundred nanometers. [1—4] Over the past two decades, the development of nanoscience and technology has created various nanostructures in forms such as nanoparticles [5—7], nanowires [8—10], nanotubes [9,11,12], nanobelts [13,14], and assembling thereof, for example, oxide aggregates [15,16]. A predominant feature of the nanostructures is that the size of their basic units is on nanometer scale (10^{-9} m). The nanostructured materials therefore present an internal surface area significantly larger than that of bulk materials. The nanoscale size may also affect the behavior of electrons transporting in nanostructures in view of a limit to the electron mean free path. This is called *quantum confinement effect*. [17—19] On the optics side, by forming photonic band gap, periodic nanostructures (known as photonic crystals) also show to be special in light manipulation and management through generating *optical confinement* or *photonic localization*. [20—23] These unique properties enable nanomaterials to

* Corresponding author.
E-mail addresses: qfzhang@u.washington.edu (Q. F. Zhang), gzcao@u.washington.edu (G. Z. Cao).

1748-0132/$ — see front matter © 2010 Elsevier Ltd. All rights reserved.
doi:10.1016/j.nantod.2010.12.007

have received considerable attention and been extensively investigated for applications in electronic, optoelectronic, photovoltaic, photocatalytic, and sensing devices.[24—28]

Solar energy is another topic that becomes increasingly hot over recent years as the fossil and mineral energy sources are approaching inevitable exhaustion in the coming fifty years. The supply of energy from the sun to the earth is gigantic; it is estimated to be 3×10^{24} J/year, which is 10^4 times more than what mankind consumes currently. In other words, covering only 0.1% of the earth's surface with a conversion efficiency of 10% would suffice to satisfy our current needs [29]. The conversion of solar energy into electricity relies on photovoltaic devices, i.e., so-called solar cells, which have undergone three generations with an evolution from the initial single silicon solar cells [30] to the second generation solar cells based on semiconductor thin films [31,32] and, now, the third generation solar cells represented by dye-sensitized solar cells (DSCs) and organic semiconductor solar cells [33—36]. Compared with the first and second generation solar cells based on conventional semiconductor materials with conversion efficiencies of ~20—30%, currently the third generation solar cells still demonstrate efficiencies relatively low [37,38]. However, the third generation solar cells have announced a lot of particularities superior to the first and second generation solar cells, for example, the compatibility with flexible substrates and low cost of materials and manufacturing [33,39—42]. As for a comparison between the organic semiconductor solar cells (with maximum efficiencies ~5—6.8%) [37,43] and the DSCs, at present, the latter, i.e., DSCs, takes obvious advantages in several aspects, such as higher efficiency, better stability, longer life time, and less dependence on the manufacturing equipments [44]. So far, the DSCs have received the maximum conversion efficiencies of ~10—11%, which may meet the requirements of most practical application [33,45—47]. Theoretical prediction of the maximum conversion efficiency of DSCs is approximately 20% [48,49].

A DSC is in essence a photoelectrochemical system, in which a dye-sensitized n-type semiconducting oxide film deposited on a transparent conductive glass substrate serves as working electrode (i.e., the so-called photoanode). A platinum-coated glass substrate placed parallel to the working electrode with a face-to-face configuration acts as counter electrode (Fig. 1). The space between these two electrodes, which is approximately 40 μm in distance, is filled with a liquid or solid electrolyte that plays a role of conducting media. The light irradiates from the working electrode side, passes through the transparent electrode, finally reaches the photoanode and gets absorbed by the dye molecules adsorbed on the oxide. The optical absorption occurring in dye molecules involves an electron transit process from the highest occupied molecular orbital (HOMO) to the lowest unoccupied molecular orbital (LUMO) [34]. The photogenerated electrons then transfer from the dye molecules to the oxide and diffuse to the transparent conducting film of the collector electrode, which is connected to the external circuit. Within a circle process, the oxidized dye molecules are reduced by the electrons in electrolyte and, simultaneously, the electrolyte is regenerated by the electrons injected from the counter electrode [50]. In DSCs, dye molecules adsorbed on the oxide play a role of ''antenna'' for photon capturing. For this reason, accompanying with the development of DSCs, organic dyes have been intensively studied with a focus on increasing the extinction coefficient and extending the optical absorption spectrum [51—57]. A variety of organic dyes used for DSCs can be found in literature, such as N3 [58], N719 [59], black dye [60], K8 [57], K19 [61], CYC-B11 [62], and C101 [63]. Some of them are already commercially available.

While the studies of the dyes are underway, on the oxide film side, the development of nanotechnology has opened a door to tailoring the materials and creating various nanostructures. The basic benefit of employing nanostructures in DSCs is that the photoelectrode films constructed with nanostructures are highly porous. It is therefore, compared

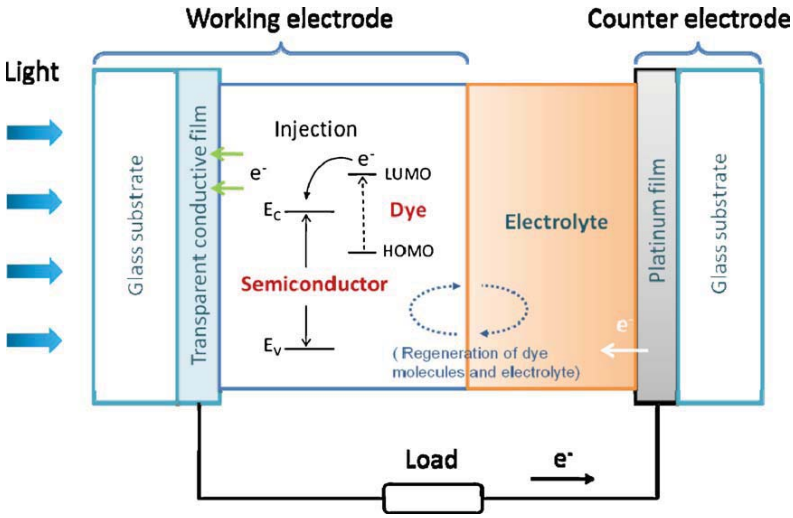

Figure 1 Outline of a dye-sensitized solar cell constructed with a working electrode consisting of dye-sensitized semiconducting oxide film, a counter electrode made of platinum-coated glass substrate, and electrolyte filled between the working and counter electrodes.

to bulk material, nanostructures forming photoelectrodes can offer a larger surface area for dye adsorption, contributing to optical absorption and leading to an improvement in the solar cell conversion efficiency. Among different nanostructures, nanoparticles have been most widely studied for use in DSCs to form photoelectrode film [64,65]. This is because, to a large extent, the films comprised of nanoparticles can give a high specific surface area. A film consisting of 15-nm nanoparticles with a thickness of 10 μm has been demonstrated to have an internal surface area as high as 780 cm^2 for each 1 cm^2 of geometric surface [64]. Another reason is probably from the ease of fabrication of nanoparticles through using simple chemical solution methods.

Nanoparticles are advantageous in providing large surface area, however the existence of numerous boundaries in the nanocrystalline films has been regarded as an unfavorable factor that may increase interfacial charge recombination happened between the photogenerated electrons and the positive species in electrolyte. Employing one-dimensional nanostructures in DSCs is an attempt to figure out this problem based on a consideration that the one-dimensional nanostructures such as nanowires, nanorods and nanotubes can provide direct pathways for electron transport from the site occurring electron injection to the conducting film of collector electrode [64]. As such, it is expected to get electron transport faster than in nanocrystalline film. This has been evidenced by experiments which reveal that the electron transport in photoelectrode comprised of single crystal nanowires is even 100 times faster than that in the case of nanocrystalline film [66]. A fast electron transport may lower the opportunity of photogenerated electrons to react with the positive species in the electrolyte and, therefore, significantly suppress the interfacial charge recombination [67,68].

Oxide aggregates are another important nanostructure reported recently with application in DSCs. The oxide aggregates are typically assembled by nanoparticles or other nanomaterials to form submicron-sized spheres [69,70]. Since the size is comparable to the wavelengths of visible light, the aggregates have been shown to be able to generate effective scattering to the light in solar spectrum. In regard of light scattering, different from those large particles (about 400 nm in diameter with a solid inner core) used in conventional DSCs, the aggregates consisting of nanomaterials possess a highly porous structure and, therefore, they on one hand play a role of light scatterers, and on the other hand they can simultaneously serve as supporting matrix for dye adsorption. In other words, while achieving light scattering, the aggregates would not result in noticeable loss in the internal surface area of the photoelectrode film. A use of aggregates of ZnO nanoparticles has demonstrated a more than doubled increase in the DSC conversion efficiency in comparison to the photoelectrode made of dispersed nanoparticles [69]. Employing an aggregate structure of TiO_2 is anticipated to be possibly able to make a breakthrough of the DSC solar cell efficiency (~11% to date) in view of a better conjunction of the TiO_2 with ruthenium-based dyes [69] and a decrease in the charge recombination as what will be mentioned in the Outlook section of this paper. The present paper reviews the use of nanostructures in DSCs. According to the dimension and structural features, the nanostructures are classified into (1) nanoparticles, which offer large surface area to photoelectrode film for dye-adsorption, however have recombination problem due to the existence of considerable grain boundaries in the film, (2) core—shell structures, which are derived from the nanoparticles with a consideration to reduce the recombination by forming a coating layer, but have been proved to be less effective and lack of consistency and reproducibility, (3) one-dimensional nanostructures such as nanowires and nanotubes, which are advantageous in providing direct pathways for electron transport much faster than in the nanoparticle film, however face drawback of insufficient internal surface area of the photoelectrode film, leading to relatively low conversion efficiency, and (4) three-dimensional nanostructures, among which oxide aggregates are addressed to be a potentially promising structure which may possibly achieve efficiency higher than the record, based on a consideration that the aggregates may simultaneously provide large surface area and generate light scattering and, therefore, they allow for making thinner photoelectrode film than usual, as such, to reduce the charge recombination in DSCs.

This review aims to demonstrate that the DSC performance is closely related to the structure of photoelectrode film. A rational design of the photoelectrode structure may lead to optimal light harvesting and electron transport. Aside from the creation of new organic dyes that is a direct way of improving the DSC efficiency, the tailoring of materials for a defined purpose is herein also emphasized to be an important way of speeding up the development of DSCs.

Nanoparticle photoelectrodes providing large surface area for dye adsorption

DSCs originate from photoelectrochemical systems appearing in 1950s. At that time, working electrode of the cells mostly employed group IV (such as silicon) or III—V semiconductors in respect that these materials had narrow band gap and therefore might absorb visible light effectively [71—73]. However, the feature of narrow band gap of the group IV or III—V semiconductors was found to be able to cause a severe corrosion problem to the working electrode under light irradiation [74]. This had driven the emergence of oxide semiconductors such as ZnO, TiO_2, and SnO_2 with wide band gap for use as the working electrode material in the early 1960s [75—78]. However, another problem came out with these wide band gap oxides that they show a poor response to the light in visible region. Such a predicament got figured out finally till the advent of dye-sensitized photoelectrodes, in which the wide band gap oxides were coated with organic dyes for extension of the optical absorption into visible region. A purposed design of the dye molecules allows a chemisorption on the oxides and an electron injection for photogenerated electrons to transfer from the dye molecules to the oxides [77—79]. This process is shown in Fig. 2 and can be specifically denoted as [74,79]

$$D + h\nu \rightarrow D^- \quad (1)$$

$$D^- \rightarrow D^+ + e^-_{CB}\ (\text{semiconductor}) \quad (2)$$

where D, D^*, and D^+ are the energy levels of dye molecules corresponding to ground, excited, and oxidized states, respectively, $h\nu$ is the energy of incident photons, and $e_{CB}{}^-$

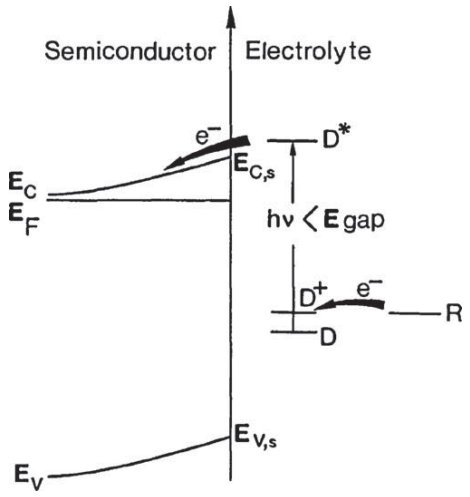

Figure 2 Schematic energy diagram of the photovoltaic effect for an n-type semiconductor in an electrolyte sensitized with an organic molecule having energy levels D, D^*, D^+ corresponding to the ground, excited (triplet or singlet) and oxidized states. '$h\nu < E_{gap}$' means the energy of incident photons is smaller than the band gap of semiconductor. The level R symbolizes the energy of a regenerating species in the electrolyte which assures reduction of the molecules back to its ground state. E_C, E_V and E_F denote the bottom of the conduction band, the top of the valence band, and the Fermi level of semiconductor, respectively [74].

denotes the electrons in the conduction band of semiconductor.

In a dye-sensitized photoelectrode, dye molecules play a critically important role in absorbing the incident photons and then generating photoexcited electrons, which finally transfer to the oxide through an electron injection. To well fulfill these functions, the dye molecules must simultaneously meet several requirements, including (1) forming chemisorption bonds with the oxide, (2) large extinction coefficient and broad absorption spectrum in the visible region, (3) suitable excited state energy level relative to the conduction band of the oxide, (4) sufficient life-time at excited state so as to allow for effective electron transfer, and (5) long term stability for many million cycles [79]. Based on these understandings, considerable efforts had been made on organic dyes since 1970s [78,80—83]. However, even though a fruitful development of dyes and the use of photoelectrode films with rough surface, such as sintered ZnO particles [74,84] and textured TiO_2 [85], the efficiencies of DSCs had hovered at a level below 3% for a long time [84] the reason was that the photoelectrode could not achieve sufficient dye adsorption due likely to low surface area of the photoelectrode film. Use of multilayer dye adsorption had been also proved to be unsuccessful for the increase of optical absorption, because of the fact that only monolayer or submonolayer of the dye molecules adsorbed on the oxide contributes to the electron injection.

An impressive breakthrough of DSCs, as is well known, was made by Grätzel et al. in 1991 using semiconductor films consisting of nanometer-sized TiO_2 particles sensitized with a trimeric ruthenium complex, announcing overall conversion efficiencies of 7.1—7.9% [64]. On one hand, such an achievement of high conversion efficiency is a result of use of a newly developed dye at that time, $RuL_2(\mu\text{-}(CN)Ru(CN)L_2')_2$, L = 2,2′ bipyridine-4,4′-dicarboxylic acid, L′ = 2,2′-bipyridine), which possesses high extinction coefficients and broad absorption spectrum with the onset at 750 nm. On the other hand, the use of crystalline nanoparticles (Fig. 3a) to form photoelectrode film is also a critically important reason that introduces a way of yielding an extremely large internal surface for dye adsorption [87]. The superiority of nanoparticles in creating large surface was demonstrated by a comparison between a flat film and a 10-μm-thick film that consisted of nanoparticles with an average size of 15 nm. The latter, nanoparticle film, showed a porosity of 50—65% and gave rise to almost 2000-fold increase in the surface area. In addition to the film constructed with nanoparticles offering a large internal surface, on the material side, the anatase TiO_2 with exposed (1 0 1) planes is also a key factor by reason of a good connection between the TiO_2 and ruthenium-based dye molecules, which enables (1) the dye molecules to form high density monolayer chemisorption on the nanoparticle surface, and (2) the electrons in dye molecules to inject into semiconductor highly efficiently (Fig. 3b) [86,88].

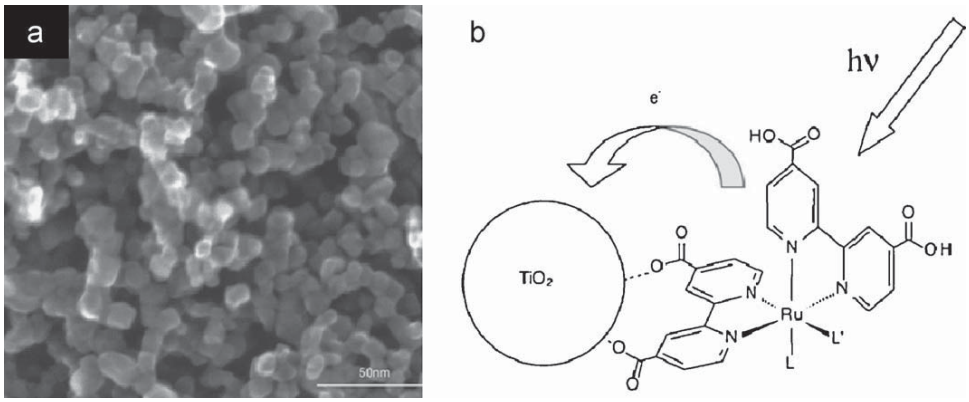

Figure 3 Dye-sensitized nanoparticle photoelectrode. (a) SEM image a TiO_2 nanoparticle film [25], and (b) adsorption of a dye molecule on TiO_2 via two of its four carboxylate groups. L and L′ represent substituted pyridines in the dye molecule, cis-[$Ru(dcbH_2)_2LL'$] [86].

During the past two decades, a number of new types of dyes, such as N3, N719, N749 (the so-called black dye), etc. [86,89—91] have been developed. These dyes greatly extended the absorption threshold of photoelectrode, leading to the receivable of high conversion efficiencies up to ~10—11% on DSCs.[29,92] Besides TiO_2 nanoparticles, other forms of TiO_2 nanostructure such as nanotubes and nanowires, and other nanostructured oxides such as ZnO [93,94], SnO_2 [94—96], Nb_2O_5 [97,98], $SrTiO_3$ [99], and Zn_2SnO_4 [100] have been also extensively studied for application in DSCs. However, up to now, most successful DSCs are till based on TiO_2 nanoparticles owing to their integrated advantage in porosity, dye adsorption, charge transfer, and electron transport [46,101]. However, despite all these, as it would be shown, those nanostructures rather than TiO_2 nanoparticles have else delivered a lot of new phenomena and concepts regarding the electron transport and light manipulation in DSCs. This gives a good source of knowledge to the existing TiO_2-based DSCs for further improvement in the performance.

Core—shell structure photoelectrodes suppressing interfacial charge recombination

Interfacial charge recombination is a problem that exists in DSCs and causes a loss of photogenerated electrons [103]. The recombination predominantly results from a reaction between the photogenerated electrons and the redox species in electrolyte; this process can be represented by $2e^- + I_3^- \rightarrow 3I^-$, where I^- and I_3^- denote the redox species in most often used electrolyte [67]. In DSCs, the interfacial charge recombination affects the open circuit voltage by decreasing the concentration of electrons in the conduction band of semiconductor [58,65,102], and affects the photocurrent by decreasing the forward injection current [65]. Interfacial charge recombination can be especially serious in the case of photoelectrode film consisting of nanoparticles, by reason that (1) the nanoparticle film gives a large internal surface and therefore may increase the probability of charge recombination due to an equally large semiconductor/electrolyte interface, and (2) the small size of individual nanoparticles only allows limited band bending at the semiconductor surface, thus there is no electric field that can assist the separation of the electrons in the semiconductor [104,105]. Core—shell structure were developed and applied to DSCs with a consideration of suppressing the interfacial charge recombination.

The core—shell nanostructures are a class of combinatorial system which is typically comprised of a core made of nanomaterials such as nanoparticles, or nanowires/nanotubes, and a shell of coating layer covering on the surface of core nanomaterials. Use of core—shell nanostructures to lower the charge recombination is based on a hypothesis that a coating layer may build up an energy barrier at the semiconductor/electrolyte interface and, thus, retard the reaction between the photogenerated electrons and the redox species in electrolyte. As for the case of nanoparticles, there two approaches have been developed to create core—shell structure. [103] One involves a first synthesis of nanoparticles and then fabricating a shell layer on the surface of nanoparticles. This leads to the formation of core—shell structured nanoparticles, with which the photoelectrode film is prepared then. Such an approach builds up a photoelectrode structure like what is shown in Fig. 4a, i.e., an energy barrier is formed not only at the nanoparticle/electrolyte interface but also between the individual core nanoparticles. In another approach, differently, the photoelectrode film comprised of nanoparticles is prepared prior to the deposition of shell layer, receiving a structure as show in Fig. 4b. The latter approach is obviously advantageous in electron transport that happens within single material, but there is usually a challenge in the fabrication of shell layer regarding a complete penetration and ideal coating of the shell material [104].

In core—shell nanostructure, to establish an energy barrier at the semiconductor/electrolyte interface, it requires that the conduction band potential of the shell material is more negative than that of the core material. As such, the back electron transport is retarded and the interfacial recombination can be reduced. A practical utilization of core—shell structure, however, was found to affect the solar cell performance in an uncertain and complicated way. Diamant et al. [102,103] and Chen et al. [105] ever performed a series of investigations on different systems that consisted of a nanoporous TiO_2 film coated with oxides such as Nb_2O_5, ZnO, $SrTiO_3$, ZrO_2, Al_2O_3 and SnO_2. The results revealed that, compared to photoelectrode made of bare TiO_2 nanoparticles, the use of Nb_2O_5 shell might increase both the open circuit voltage and the short circuit current, eventually giv-

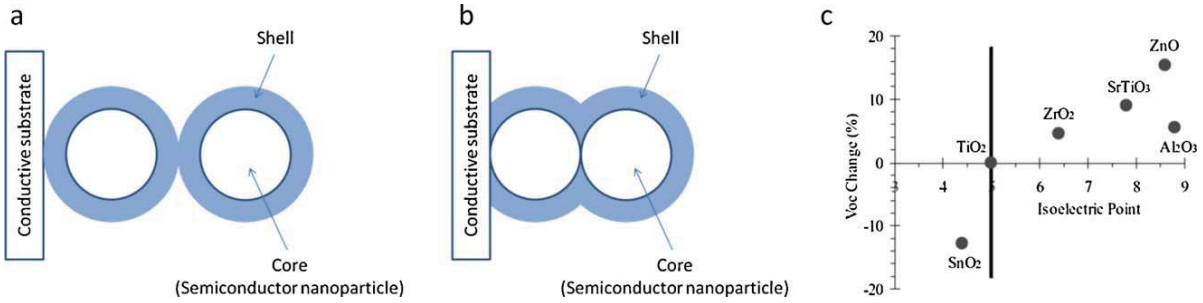

Figure 4 Core—shell structures used in DSCs. (a) The shell layer is formed prior to the film deposition, (b) the shell layer is coated after the film deposition, and (c) the dependence of open circuit voltage change on the isoelectric point of shell material in a DSC [103]. (The shell material with higher isoelectric point than that of TiO_2 may establish a surface dipole directed toward the TiO_2 core, and thus negatively shift the conduction band of TiO_2.)

ing rise to an enhancement in the solar cell efficiency by about 37%. Considering the onset of conduction band of the Nb_2O_5, $\sim -0.6\,V_{NHE}$, which was more negative than the $\sim -0.42\,V_{NHE}$ for TiO_2, it was inferred that an energy barrier was formed at the surface of TiO_2 nanoparticles. By lowering the back recombination rate of photogenerated electrons in TiO_2, the energy barrier led to an increase in both the open circuit voltage and the observed photocurrent (Note that the observed photocurrent is the difference between the forward photocurrent and the photocurrent caused by the back recombination.).

Different from Nb_2O_5 that established an energy barrier, a coating of other materials like ZnO, $SrTiO_3$, ZrO_2, Al_2O_3, and SnO_2 was suggested to yield a surface dipole layer. Such a dipole layer might shift the conduction band of the TiO_2, causing an increase in the open circuit voltage in the case of ZnO, $SrTiO_3$, ZrO_2 and Al_2O_3 however a decrease in the case of SnO_2. This was attributed to the direction of the surface dipole, which was found to depend on the isoelectric point of the shell material. As shown in Fig. 4c, for the oxides such as ZnO, $SrTiO_3$, ZrO_2 and Al_2O_3 with isoelectric points higher than that of the TiO_2 (~5–5.5), a surface dipole layer was created toward the TiO_2, leading to a negative shift of the conduction band of the TiO_2. This resulted in an increase in the open circuit voltage of the cells. However, in experiment, a decrease in the photocurrent was observed. This suggested that, unexpectedly, the formation of a dipole layer might accelerate the back recombination. Therefore, for these core–shell nanostructures, the resulting efficiency of the solar cell depended on a competition between the increase in open circuit voltage and the decrease in short circuit current. As a result, for the ZnO, $SrTiO_3$, and Al_2O_3, the core–shell structure produced ~15% enhancement in the overall conversion efficiency. However, for the ZrO_2 shell, it showed an decrease in the overall efficiency by ~11% [103]. For SnO_2, it possessed the isoelectric point lower than that of TiO_2. The shell of SnO_2 therefore created a dipole layer being opposite to the TiO_2, leading to a decrease in both the open circuit voltage and short circuit current.

However, there is still a debate so far regarding the effects and mechanism of shell layer. For example, in another study that compared SiO_2, ZrO_2 and Al_2O_3 while coating on TiO_2 nanoparticles, among these oxides, the Al_2O_3-coated TiO_2 nanoparticles achieved the maximal increase in DSC efficiency by ~35% [104]. Based on the experimental observation showing an increase in both the open circuit voltage and the short circuit current, it was explained that the Al_2O_3 shell established an energy barrier at the semiconductor/electrolyte interface. Different from either the surface dipole or the energy barrier mechanism, another opinion believes that a coating of Al_2O_3 on the TiO_2 may receive more basic surface in view of high isoelectric point of the Al_2O_3 (~9.2) and therefore the improved solar cell performance arises from better dye adsorption [104,106]. In addition, in the case of ultrathin shell (≤1 nm), a passivation mechanism was proposed to explain the compression of back charge transfer [107].

To retard the back recombination of photogenerated electrons, it is expected to build up an energy barrier using a shell material with the conduction band edge more negative than that of the core material, as shown in Fig. 5. However, the barrier height is limited by a consideration that the energy barrier would not influence the electron injection from the dye molecules to the core oxide. This gives a theoretical criterion for the shell material that should have the conduction band edge which is located between the conduction band edge of the core material and the excited state potential of the dye, as shown in Fig. 5b. In this case, the electron injection takes place without mounting an energy barrier. Core–shell nanostructures such as SnO_2/TiO_2 [108], SnO_2/ZnO [109], and TiO_2/Nb_2O_5 [97] are examples designed according to such a criterion and used for DSCs to purposely lower the charge recombination, however only receive limited success.

From the discussion above, it can be clearly seen that there is still a lot of uncertainty with regard to the effects of core-shell structures used in DSCs. The enhancement by use of a shell layer is sometimes farfetched, and even shows inconsistency in literature. This is probably due to the difficulty of creating a shell layer with ideal thickness, coverage, crystallinity, and electrical coupling to the semiconductor core. Research on this topic is still facing challenges on both scientific and technical aspects.

One-dimensional (1D) nanostructure photoelectrodes offering direct pathways for electron transport

Drawbacks of nanoparticle films

Nanoparticle films have been regarded as a paradigm of porous photoelectrode for use in DSCs. However, the nanoparticle films are not thought to be ideal in struc-

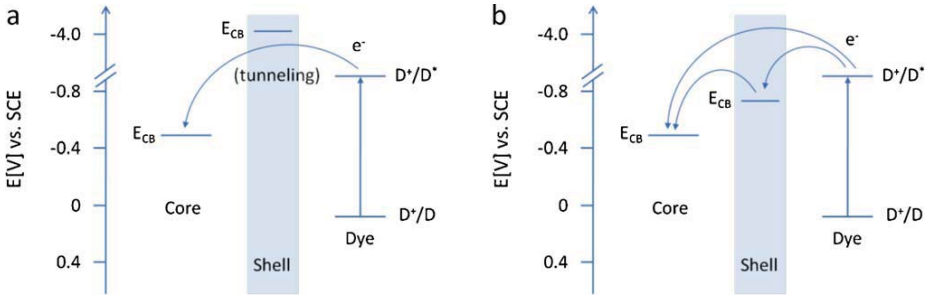

Figure 5 Energy level structure of a core–shell structure in DSCs: (a) the edge of conduction band of the shell material is higher than the excited state of dye molecule, and (b) the edge of conduction band of the shell material is located between the excited state and the conduction band edge of the core material.

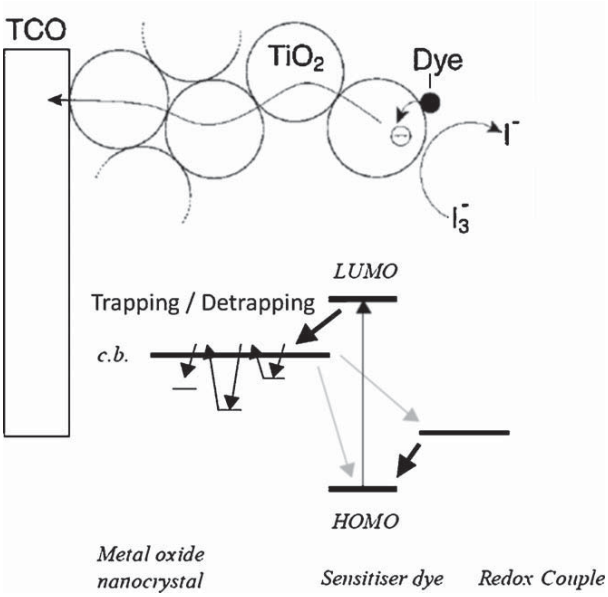

Figure 6 Electron transport in a nanoparticle film suffering a trapping/detrapping process [110,111].

ture with regard to electron transport. The first non-ideality results from the lack of a macroscopic electrostatic potential gradient in the film due to the fact that the film is permeated with a concentrated electrolyte [34]. Therefore, the electron transport in the nanoparticle film is dominated by a process of diffusion instead of drift; the latter a common way in p—n junction solar cells for carrier separation in the presence of an electric field. The second non-ideality comes from the fact that the electron transport in a nanoparticle film undergoes a trapping and detrapping process, i.e., the injected electrons can be captured by the trap states and, however, can be again thermally emitted back to the conduction band (Fig. 6) [110,111]. The trapping, which may result in an energy loss to the injected electrons, is particularly serious in the case of nanoparticle film because of numerous grain boundaries existing in the nanoparticle film [112]. This is in agreement with a measurement of the electron diffusion coefficient of TiO_2 nanoparticle film, $5 \times 10^{-5}\,cm^2\,s^{-1}$, which is more than two orders of magnitude smaller than that obtained for bulk material [113—115]. The electron diffusion coefficient determines the electron diffusion length by $L_n = \sqrt{D_n \tau_n}$, where L_n is the electron diffusion length, D_n is the electron diffusion coefficient, and τ_n is the electron lifetime [116]. For nanoparticle films, the typical electron diffusion lengths are ~10—14 μm. This is the reason that an optimal film thickness for the nanoparticle photoelectrode is around ten several micrometers and, moreover, a simply thickening of the nanoparticle film has been proved to be unsuccessful for an increase of dye adsorption or optical absorption. However, in this regard, one-dimensional nanostructures have been shown to be advantageous in offering direct pathways for electron transport and therefore giving electron diffusion length larger than in the nanoparticle films [66,116—119].

ZnO nanowires

ZnO nanowires were reported by Law et al. for the first time to demonstrate that one-dimensional nanostructures might provide direct pathways for electron transport in DSCs [66]. The experiment was purposely designed to grow ZnO nanowires with a high aspect ratio so as to attain a nanowire film with high density and sufficient surface area (Fig. 7a and b). A ~25-μm-thick film consisting of ZnO nanowires in diameter of ~130 nm was mentioned to be able to achieve a surface area up to one-fifth as large as a nanoparticle film used in the conventional DSCs. The superiority of ZnO nanowires for DSC application was firstly demonstrated by their high electron diffusion coefficients, $0.05—0.5\,cm^2\,s^{-1}$, which are several hundred times larger than those of nanoparticle films. Larger diffusion coefficient means longer diffusion length. In other words, the photoelectrode made of nanowires allows for thickness larger than that in the case of nanoparticles. This can compensate for the insufficiency of surface area of the photoelectrode film while it comprises nanowires.

Besides showing a large diffusion coefficient, the nanowires were also demonstrated to be advantageous in charge collection. This was illustrated by explaining that the size of the individual nanowires was much larger than the Debye—Hückel length of ZnO (~4 nm). Therefore, an internal electric field was established within the nanowires and was able to assist the carrier collection by separating injected electrons from the surrounding electrolyte and

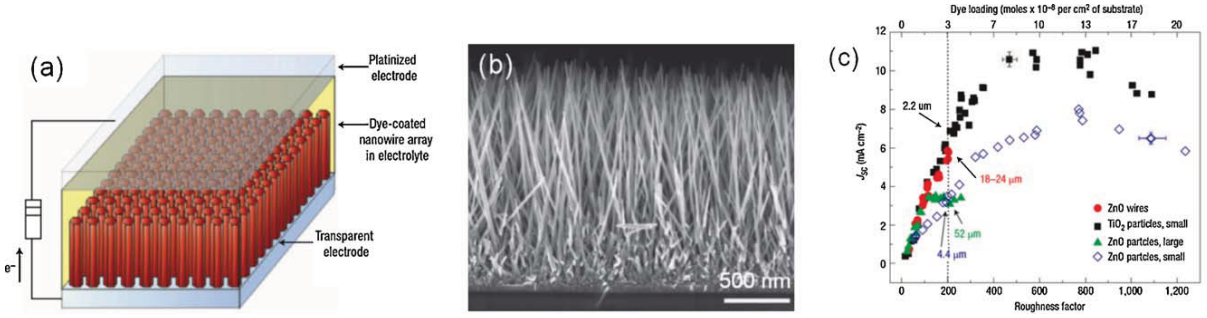

Figure 7 ZnO nanowire dye-sensitized solar cell [66]: (a) schematic diagram of the cell, (b) scanning electron microscopy image of ZnO nanowire array, and (c) comparative performance of nanowire and nanoparticle cells. At a roughness factor of 200, the nanowire cell generates photocurrent 55—75% higher than the ZnO nanoparticles and comparable to the TiO_2 nanoparticles.

sweeping them toward the collecting electrode. Shown in Fig. 7c depicts that the charge collection efficiencies of ZnO nanowire photoelectrodes, ~55—75%, are much higher than those of photoelectrodes made of ZnO nanoparticles (Fig. 7c).

The ZnO nanowires were also emphasized to be superior to nanoparticles in electron injection kinetics. This is based on a measurement of the time constants of electron injection, indicating 3 ps for nanowires and 200 ps for nanoparticles. The faster response of ZnO nanowires was ascribed to the 95% exposed (1 0 0) crystal plane of the nanowires, which was more favorable to yielding chemical bonding with the dye molecules in comparison to the nanoparticles. For all these merits in geometry and electrical property, ZnO nanowires have been suggested to be a promising photoelectrode material which provides direct pathways for a rapid electron transport.

TiO_2 nanowires

TiO_2 nanowires are another important one-dimensional nanostructure that has also attracted a lot of interests regarding an application in DSCs [116,117]. Hydrothermal growth has been reported to be a novel method for synthesis of TiO_2 nanowire array on FTO glass substrate. In this method, tetrabutyl titanate and/or titanium tetrachloride were used as the precursor, to which an HCl solution was added to stabilize and control the pH of the reaction solution. Growth typically occurring at 180—220 °C for ~24 h might form nanowires 35—90 nm in the lateral dimension and ~4 μm in the length (Fig. 8a). Structural characterization revealed that these nanowires were rutile phase, and the growth was along [0 0 1] orientation with exposed (1 1 0) crystal plane (Fig. 8b). The Cl^- ions were explained to play an important role in the growth of TiO_2 nanowires by attaching on the (1 1 0) plane of the TiO_2 nanocrystallites and thus suppressing the growth of this plane.

The dependence of photocurrent density on the measured potential was studied while the TiO_2 nanowires were under AM 1.5 illumination, revealing a saturated photocurrent at the bias of approximately −0.25 V (vs reference electrode) (Fig. 8c). Compared with a positive bias in the range of 0.5—1 V needed in the nanoparticle electrode to completely separate the photogenerated electron—hole pairs, such a low bias indicated that the nanowires possessed a low series resistance and had more effective capability of facilely separating the photogenerated charges. This is in agreement with what is presented in the incident photo to collected electron (IPCE) spectrum of TiO_2 nanowires (inset of Fig. 8c), in which the efficiency is shown to reach a maximum of approximately 90%, implying a low charge recombination in the nanowire/electrolyte system. Test of

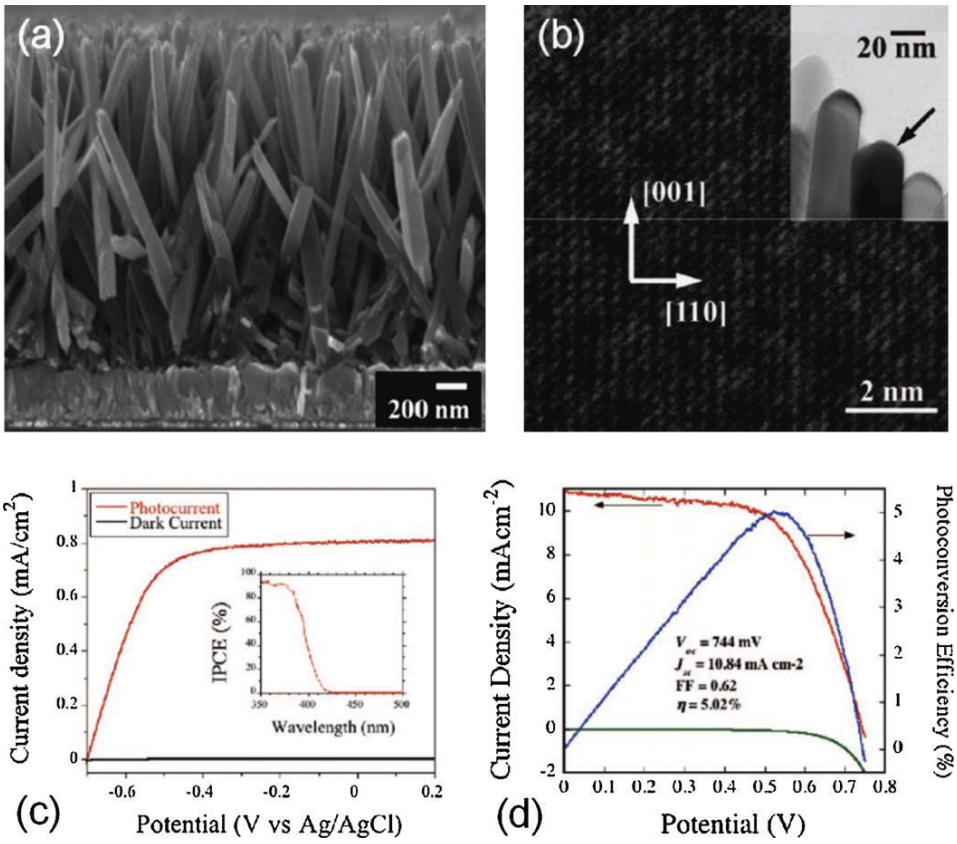

Figure 8 DSCs with TiO_2 nanowires [116,117]: (a) cross-sectional SEM image of TiO_2 nanowire array grown on transparent conductive substrate, (b) TEM image illustrating the [0 0 1] orientation of TiO_2 nanowires, (c) photocurrent density of a TiO_2 nanowire photoelectrode film as a function of measured potential in 1 M KOH under AM 1.5 illumination; the inset shows the IPCE spectrum, and (d) photovoltaic response of a TiO_2 nanowire solar cell.

the solar cell performance of the TiO_2 nanowires with a standard DSC configure revealed an overall conversion efficiency of 5% (Fig. 8d), which is obviously much higher than those of 1.2—1.5% reported for ZnO nanowires even with length up to 40 μm [66,118]. This most likely results from a better coupling of the nanowires of TiO_2 with the ruthenium-based dye molecules, whereas it is well-known that the ZnO lacks stability in an acid dye solution and therefore may form a Zn^{2+}/dye complex on the surface which seriously retards the electron injection [118—120].

A comparison of the solar cell performance between TiO_2 nanowires and nanoparticles that were also rutile phase presented an interesting result, i.e., the efficiency achieved by the TiO_2 nanowire film in 2—3 μm thick was higher than that obtained for the nanoparticle film in 5 μm thick [88]. This is a good evidence that the one-dimensional nanostructures may offer better charge transport than the nanoparticles. A further increase in the conversion efficiency most likely relies on the development of new fabrication techniques that can achieve longer TiO_2 nanowires.

Besides TiO_2 nanowire array, randomly oriented TiO_2 nanowires have been also studied for DSC application in view of high porosity of the film consisting of nanowires [121—123]. Electrospinning is a facile approach that has been reported to directly produce TiO_2 nanowires on FTO glass substrate. The solution for electrospinning typically contains titanium alkoxide, acetic acid, polyvinylpyrrolidone (PVP), and ethanol. The product needs to be sintered at 500 °C to remove the organics and convert to anatase TiO_2. A treatment of the TiO_2 nanowires with tetrahydrofuran (or hot-pressing) was mentioned to be able to improve the adhesion of the nanowires on FTO glass substrate. With the TiO_2 nanowires prepared and treated as such, a DSC efficiency as high as ~5.8% has been obtained for a photoelectrode comprised of nanowire film in 20 μm thick [121,122].

TiO_2 nanotubes

Nanotubes are a class of very important one-dimensional nanostructure since their hollow structure may usually give surface area larger than that of nanowires or nanorods. Anodization has been a method that is intensively employed for the fabrication of TiO_2 nanotubes [124—126]. The fabrication involves a simple anodic oxidation of titanium foil in a fluoride-based solution at a constant potential [127,128]. The TiO_2 nanotubes formed on the supporting titanium foils (Fig. 9a) typically possess inner diameter in the 20—30 nm range, wall thickness in the order of ten several nanometers, and length that ranges from several tens micrometers to even millimeter, predominantly depend-

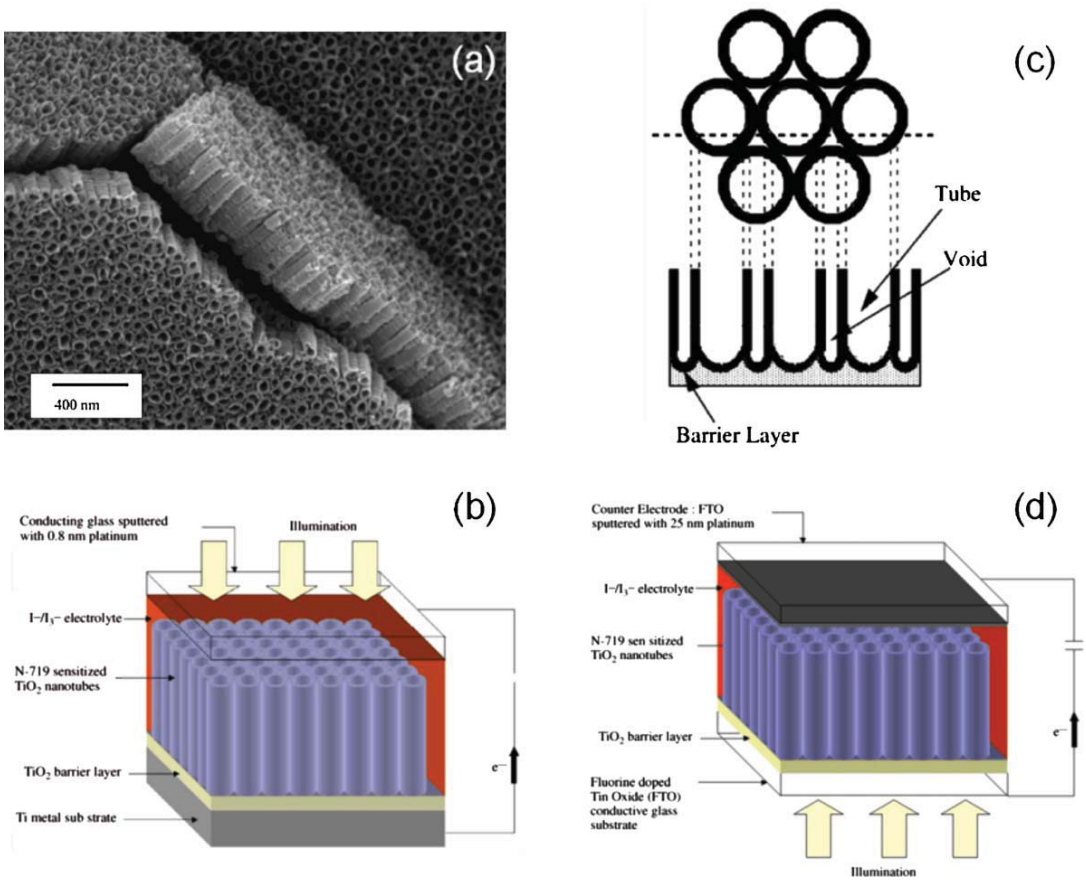

Figure 9 TiO_2 nanotubes prepared with an anodization method and their application in DSCs [127,139]: (a) morphology of the TiO_2 nanotube array, (b) growth mechanism of the nanotubes and formation of a barrier layer under the nanotube film, (c) back-side illumination and (d) front-side illumination structures of the DSCs made of TiO_2 nanotube array.

ing on the composition of electrolyte, applied bias, and growth time [129—133]. For TiO_2 nanotubes prepared with the anodization method, annealing in air at elevated temperature such as 450 °C is necessary to transform the crystal structure from amorphous to anatase phase [134].

(i) Back-side illumination

Macák et al. reported for the first time that anodic TiO_2 might have a DSC application in 2005 [135]. The configuration of this kind of structured solar cells typically adopts a back-side illumination geometry, as shown in Fig. 9b, by reason of non-transparency of the titanium foil. In operation, the light comes from the side of platinum electrode, which is made of a 0.8-nm-thick platinum film coated on a glass substrate and is nearly transparent. With such structured solar cells, a maximum of 4.24% efficiency has been reported while the photoelectrode film is comprised of ~6 μm long TiO_2 nanotubes [136]. An increase in the length of the nanotubes, for example, to 20 μm was found to make no significant contribution to the conversion efficiency [137,138]. This probably results from the existence of an electrically insulating barrier layer, ~1 μm thick, between the nanotubes and the conducting titanium foil (Fig. 9c) [127], which gives rise to increase in the series resistance of the cell as the nanotubes grow longer.

(ii) Front-side illumination

The biggest problem with the back-side illumination geometry is that the light has to pass through the electrolyte before reaching the TiO_2 electrode. It therefore unavoidably causes a loss of incident light. A way to overcome this drawback is to directly prepare the TiO_2 nanotube array on a transparent conductive substrate such as FTO glass [140]. This gives a front-side illumination geometry same as the structure employed in traditional DSCs (Fig. 9d) [141]. The fabrication of this structured photoelectrode requires a deposition of metal titanium film on the conductive glass substrate in advance. The resulting titanium film then undergoes an anodization, resulting in the formation of nanotube structure. A consequent heat treatment at ~500 °C in oxygen is essential to converting the TiO_2 from amorphous to anatase phase with high transparency [142]. This method, however, encounters a difficulty in practice in the fabrication of high-quality titanium film thicker than 1 μm on the FTO glass substrate. As a result, the film of TiO_2 nanotube array prepared with this method has limited thickness and cannot offers a sufficiency internal surface area for dye adsorption. With a direct growth of TiO_2 nanotubes on the FTO glass substrate, so far the maximum overall conversion efficiency is approximately 2.9% obtained for a photoelectrode consisting of 360-nm-long nanotubes [139]. For this method, besides a limit to the film thickness, it else faces a problem of adhesion of the nanotubes on FTO glass substrate. Recently, a two-step fabrication technique has been invented to well figure out these problems.[143] In this technique, a layer of TiO_2 nanotube film was firstly grown on a titanium foil using an anodization method. The nanotube film was then lifted off from the titanium foil through an acid treatment and subsequently transferred onto a glass substrate, where a few drops of titanium isopropoxide was applied for an interconnection between the nanotube film and the FTO film on glass substrate. A 35-μm-thick TiO_2 nanotube photoelectrode film fabricated with this method has received a conversion efficiency as high as 7%.

(iii) Structure optimization

In addition to investigations on basic parameters such as diameter, length and density of TiO_2 nanotubes that may affect the solar cell performance, a lot of insightful studies have else attempted different ways to optimize the geometrical structure (i.e., the alignment) of the TiO_2 nanotubes toward higher conversion efficiency. For example, the technique of supercritical CO_2 drying applied to the TiO_2 nanotube films was demonstrated to be able to avoid the formation of bundles and thus reduce interfacial charge recombination rate. The transport of photogenerated electrons was therefore enhanced [144]. A pre-treatment of the titanium foil with purpose of forming a thin layer of rutile TiO_2 was shown to be effective in preventing from the formation of a disordered topping layer. The resultant nanotubes presented to be highly aligned and lead to an improvement in the solar cell performance by increasing efficiency from 2.88% to 3.05% [145]. A similar enhancement effect was also observed on aligned TiO_2 nanotubes synthesized in an electrolyte of ethylene glycol containing NH_4F while the substrate, i.e., titanium foil, was pre-treated to be covered with photoresist [146].

(iv) Bamboo-type TiO_2 nanotubes

Unlike a constant DC potential that was most often used in literature for growth of TiO_2 nanotubes, a use of AV potential was found to be able to produce TiO_2 nanotubes with

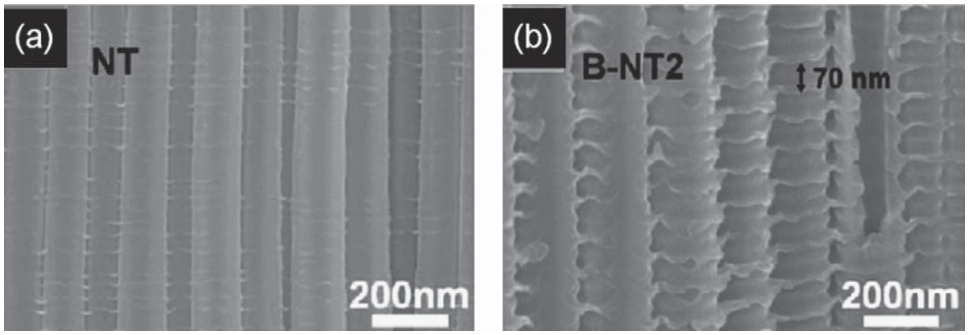

Figure 10 SEM images of smooth-walled TiO_2 nanotubes (NT) and bamboo-type TiO_2 nanotubes (B-NT2) grown with an anodization of titanium foil under DC and AV conditions, respectively [47].

a so-called bamboo-type morphology (Fig. 10) [147]. The advantage of these bamboo-type nanotubes was suggested that they presented a more porous structure and therefore might offer larger surface area for dye adsorption in comparison to those smooth-walled nanotubes created under DC condition conventionally. It was found that the morphology of the bamboo-type nanotubes in the distance between the stratification layers was adjustable by simply changing the AV pulse durations. An efficiency of ~2.96% was achieved on the bamboo-type nanotubes that were grown under AV condition with a sequence of 1 min at 120 V and 5 min at 40 V for 12 h, whereas the efficiency was only 1.90% for the smooth-walled nanotubes same in length, well demonstrating that the bamboo-type nanotubes might receive additional surface area for catching more dye molecules.

ZnO nanotubes

ZnO nanotubes have been also studied for application in DSCs. However, the conversion efficiencies so far achieved were generally low, ~1.2—1.6% [148—151]. It probably results from a fact that the length of the ZnO nanotubes is limited by the fabrication method based on an etching mechanism. A typical fabrication includes a first growth of ZnO nanorods and a consequent treatment in alkaline solution; the latter step is to convert the nanorods into nanotube structure through a chemical etching. However, during the etching treatment, an accompanying dissolution of the ZnO occurs simultaneously and thus leads to a shortening of the nanorods. This finally results in a limit to the length of received nanotubes [148]. A template method was also reported to create ZnO nanotubes through an atomic layer deposition (ALD) to fabricate ZnO in the pores of anodic aluminum oxide (AAO) membrane. However, the surface area of the ZnO nanotubes is also very low due to a limit of the available size and pore density of the AAO membranes [150,151].

Hybrid nanostructures of nanowires/nanotubes mixed with nanoparticles

Hybrid nanostructures here specifically refer to a combination of nanowires/nanotubes and nanoparticles. A straightforward consideration of using a hybrid structure in the photoelectrode film is to compensate the shortcoming of the one-dimensional nanostructures having insufficient surface area by filling up nanoparticles into the interstices of nanowire or nanotube array film. With such a configuration, the nanoparticles inserted among the nanowires or nanotubes contribute to increasing the internal surface area of the photoelectrode film, while the one-dimensional nanostructure works as a backbone to fulfill the transport of electrons received from those surrounding nanoparticles (Fig. 11a) [152].

Many examples concerning hybrid nanostructures for DSC application can be found in literature. Most of investigates were carried out on the array films of ZnO nanowires, TiO_2 nanowires, or TiO_2 nanotubes filled with ZnO or TiO_2 nanoparticles [152—156]. For instance, a fill-up of ZnO nanowire array with ZnO nanoparticles that were created with a chemical bath deposition might result in a significant increase in the overall conversion efficiency, from 0.5—0.8%

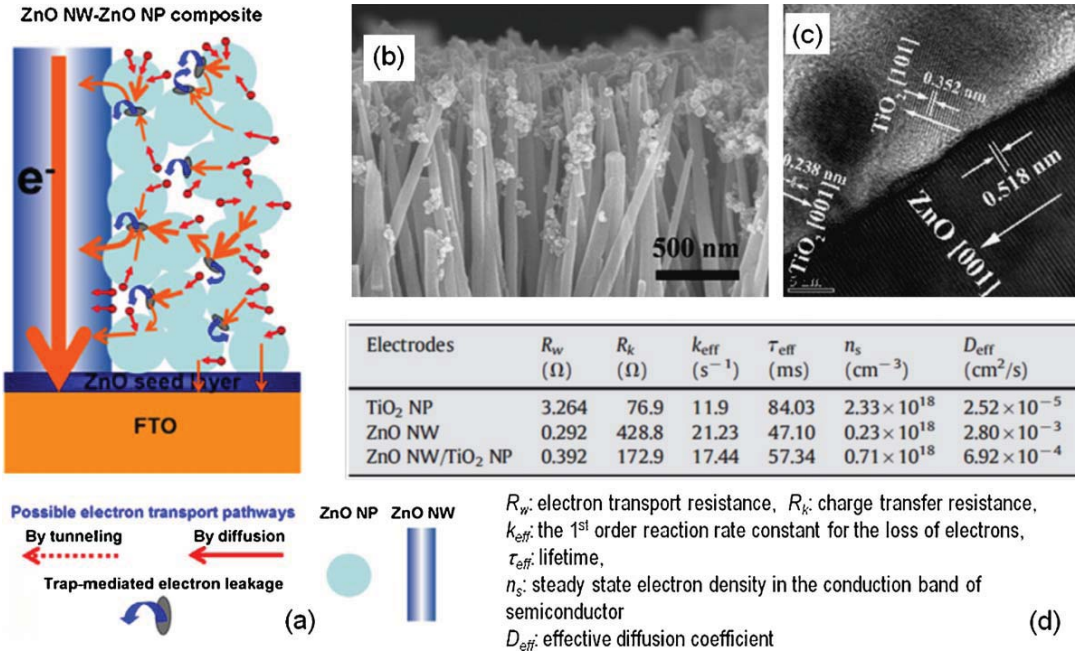

Electrodes	R_w (Ω)	R_k (Ω)	k_{eff} (s^{-1})	τ_{eff} (ms)	n_s (cm^{-3})	D_{eff} (cm^2/s)
TiO_2 NP	3.264	76.9	11.9	84.03	2.33×10^{18}	2.52×10^{-5}
ZnO NW	0.292	428.8	21.23	47.10	0.23×10^{18}	2.80×10^{-3}
ZnO NW/TiO_2 NP	0.392	172.9	17.44	57.34	0.71×10^{18}	6.92×10^{-4}

R_w: electron transport resistance, R_k: charge transfer resistance,
k_{eff}: the 1st order reaction rate constant for the loss of electrons,
τ_{eff}: lifetime,
n_s: steady state electron density in the conduction band of semiconductor
D_{eff}: effective diffusion coefficient

Figure 11 Hybrid nanostructures for application in DSCs [152,154]: (a) a schematic of hybrid structure photoelectrode with ZnO nanowires and ZnO nanoparticles, providing both direct pathways for electron transport and large surface area for dye adsorption [152], (b) SEM and (c) TEM images of ZnO nanowires with TiO_2 nanoparticles attached on the surface, and (d) fitting parameters of impedance spectra obtained for DSC photoelectrodes with TiO_2 nanoparticles, ZnO nanowires, and a hybrid of ZnO nanowires and TiO_2 nanoparticles [154].

to 2.2—3.2% [152,155]. In another study, TiO_2 nanotube array film produced on titanium foil by an anodization method demonstrated an efficiency increase from 3.81% to 5.94% while filled with ~10 nm TiO_2 nanoparticles [157]. Measurement of electron impedance spectroscopy (EIS) revealed that, as shown in Fig. 11 (insert Table), both the steady state electron density in the conduction band of semiconductor (n_s) and the effective diffusion coefficient (D_{eff}) of the hybrid structure fell between those of bare nanoparticle and nanotube electrodes [154,157]. The n_s in hybrid nanostructure electrodes higher than that in nanotube electrodes gives good evidence that the incorporation of nanoparticles may provide more surface area for dye adsorption and thus enhance the light harvesting of photoelectrode. The D_{eff} in the hybrid nanostructure electrodes presents to be larger than that in the nanoparticle electrodes. This, in turn, indicates that the use of one-dimensional nanostructures may facilitate electron transport in DSCs. A decrease in the D_{eff} of the hybrid nanostructure electrodes in comparison to bare nanotube electrodes does not bring about significant impact on the solar cell performance, because the electron diffusion length in the hybrid nanostructure electrodes (L_n = ~20—30 μm) is larger than the thickness of the photoelectrode film (~3—5 μm) [157]. A nanotube/nanoparticle hybrid structure can be also attained through a $TiCl_4$ treatment of TiO_2 nanotube array [158,159]. Such a treatment typically leads to the formation of ~3-nm nanoparticles adsorbed on the TiO_2 nanotubes, giving an increase in the conversion efficiency by approximately 40%.

Besides considerable attention paid to the nanowire and nanotube arrays, there are also lots of studies focusing on randomly orientated one-dimensional nanostructures associated with nanoparticles. A mixture of template-synthesized TiO_2 nanotubes with 2% P25 (a kind of commercially available TiO_2 nanoparticle powder provided by Degussa, Germany) was demonstrated to result in an improvement in the efficiency from 7.83% for nanotubes alone to 8.43% for the hybrid structure [160].

In another kind of hybrid structure, the major phase is nanoparticles, however the one-dimensional nanostructures such as ZnO nanowires, TiO_2 nanowires [161,162], and carbon nanotubes [162] are added in a small fraction, for example, ~0.1—20% in weight. In these structures, the function of these 1D nanostructures is, on one hand, to increase the conductivity of the photoelectrode film, and on the other hand, these 1D nanostructures are introduced to generate light scattering and thus improve the optical absorption of the photoelectrode.

Surface modification of 1D nanostructures

Surface modification, which possibly results in a core—shell structure in the case of thick coating layer, is also effective in enhancing the performance of solar cells with one-dimensional nanostructures. TiO_2 has been a common material to be coated on a variety of 1D nanostructures such as ZnO nanowires [163], SnO_2 nanowires [164], indium—tin oxide nanowires [165], and carbon nanotubes [166]. The enhancement comes from a mechanism similar to what has been discussed in Section 3 concerning nanoparticles, i.e., a surface barrier is formed to reduce the charge recombination. One example regarding ZnO nanowires coated by 10—25 nm-thick TiO_2 proposed that a radial field was established on the surface of ZnO nanowires. This increased the open circuit voltage of the solar cell and led to an enhancement in the conversion efficiency, from 0.85% to 1.7—2.1% [163]. Another investigation reported an efficiency of 4.1% for TiO_2-coated SnO_2 nanowire photoelectrode, which was almost two times higher than the 2.1% obtained for bare SnO_2 nanowires [164].

Three-dimensional (3D) hierarchical nanostructure photoelectrodes with multiple functions

Besides those nanostructures like nanoparticles, nanowires, nanotubes, and the mixtures thereof which have been most often investigated, recently three-dimensional hierarchical nanostructures appear to be used for photoelectrode in DSCs and have caught a lot of particular attention [167,168]. The advantage of three-dimensional nanostructure photoelectrodes is that they not only emphasize large surface area, but also show excellent capability in achieving highly effective light harvesting and charge transport and collection.

ZnO nanotetrapods

ZnO nanotetrapods are one of typical three-dimensional nanostructures which consist of four arms extending to different spatial orientations from a common core (Fig. 12a) [169]. ZnO nanotetrapods can be synthesized by a vapor transport deposition [169,170]. The produced nanotetrapods typically feature a structure with the arms 40 nm in diameter and 500—800 nm in length. The roughness factor of a film composed of the ZnO nanotetrapods was demonstrated to be as high as 400. ZnO nanotetrapods are of benefit to DSCs owing to their large specific surface area in view of high roughness factor and good interconnection of the arms offering multiple pathways for electron transport. A photoelectrode film consisting of the ZnO nanotetrapods (approximately 31 μm in thickness) was reported an overall conversion efficiency of 3.27%, which was generally higher than those obtained for ZnO nanowire array [66,171].

Branched nanowires or nanotubes

Branched nanostructures are derived from one-dimensional nanostructures however with a consideration to enlarge the surface area through using extended ''branches''. Typical branched nanostructures include (1) nanoflowers, (2) forest-like architecture, (3) branched nanowires, and (4) dendritic nanowires.

(1) Flower-like ZnO nanostructure (Fig. 12b) can be synthesized by a hydrothermal decomposition. The flower-like ZnO nanostructure used for DSCs presented a conversion efficiency of 1.9%. This was demonstrated to be almost 90% higher than that obtained for upstanding nanorods without branches [172]. It was explained that the extended nano-sized branches played a role in intercepting the incident light and, as such, increasing the light harvesting of the photoelectrode.

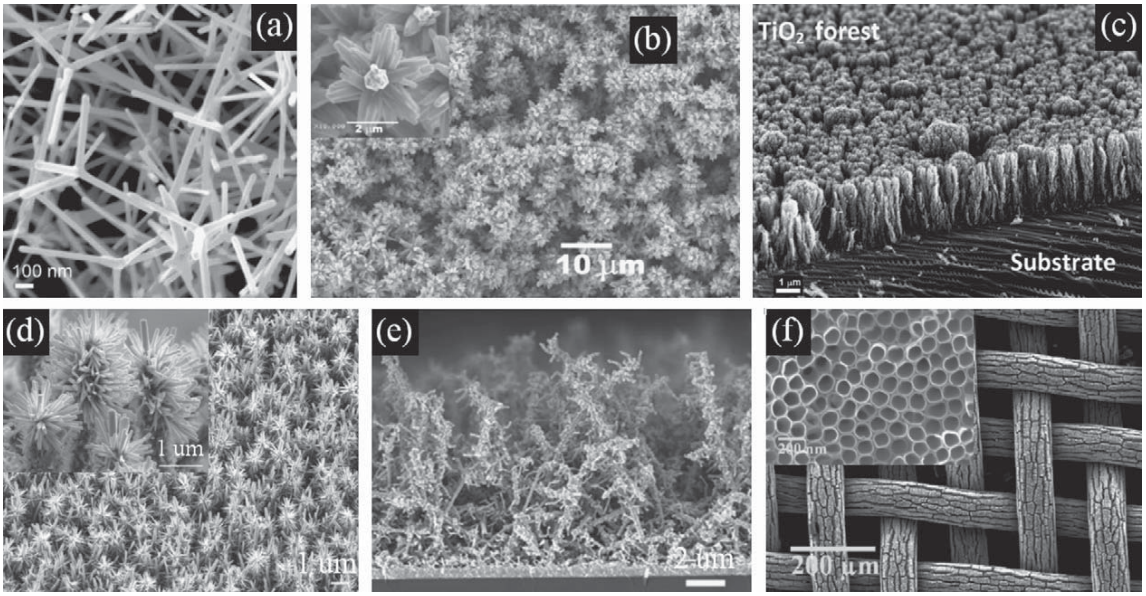

Figure 12 Three-dimensional nanostructures for DSC application: (a) ZnO nanotetrapods [169], (b) ZnO nanoflowers [172], (c) forest-like architecture of TiO_2 [173], (d) branched ZnO nanowires [174], (e) dendritic ZnO nanowires [175], and (f) TiO_2 nanotubes on titanium mesh [176].

(2) Forest-like TiO_2 film grown FTO-coated glass substrate can be prepared with a pulsed laser deposition (PLD) method [173]. The film consists of assemblies of 10-nm nanocrystalline particles of anatase TiO_2, morphologically resembling a tree with the branches approximately 40 nm in diameter and 500 nm in length (Fig. 12c). This structure provides the film with a large surface area of 86 m^2/g and high porosity, ~79%. As for solar cell performance, a 7-μm-thick photoelectrode film received 4.9% conversion efficiency (with C101 dye). Importantly, a study on the dynamics of interfacial charge transfer processes revealed that the electron life time in the forest-like film was increased by more than 1 order of magnitude in comparison to the conventional mesoporous film composed of 20-nm nanocrystalline particles. This implies that, similar to the case of nanowires, the film with forest-like morphology may also provide direct pathways for charge transport and hamper the electron recombination in DSCs.

(3) Branched nanostructures can be created by a two-step or multiple-step method. This involves a synthesis of one-dimensional nanostructures as firstly. These one-dimensional nanostructures then work as ''backbone'' to induce a further growth of sub-nanostructures on the surface, finally leading to the formation of a three-dimensional hierarchical structure. In one of examples, ZnO nanowires was prepared with a solution method and then coated with ZnO nanoparticles as seed layers [174]. The substrate with the seed-decorated ZnO nanowires was put into a diluted reaction solution for a secondary growth. This resultant nanowire branches are composed of backbone nanowires having length and diameter in the range of 7—8 μm and 150—250 nm, respectively and branches 100—300 nm in the length and 20—50 nm in the diameter (Fig. 12d). These branched nanowires indicated a conversion efficiency of 1.51%, twice higher than that for bare ZnO nanowires (without branches).

(4) Dendritic ZnO nanowires are a hierarchical structure similar to branched nanowires however with multiple-generation growth of sub-branches (Fig. 12e). A detailed procedure for fabrication of the dendritic ZnO nanowires via a MOCVD method was described by Baxter et al. [175,177] This kind of nanostructure demonstrated a DSC efficiency of 1.1%.

Mesh-based 3D photoelectrode

Mesh-based 3D photoelectrode (Fig. 12f) was reported by Rustomji et al. with an attempt to maximize the surface area of photoelectrode comprised of TiO_2 nanotubes [176]. By employing commercial metal mesh of titanium (99.5 wt% Ti), an anodization was carried out on the mesh to produce TiO_2 nanotubes on the surface of titanium fibers. Due to use of mesh as a substrate, the growth of TiO_2 nanotubes was toward different orientations. The produced mesh therefore presented a surface area much larger than that of a flat titanium foil. Solar cell constructed with such a 3D mesh with TiO_2 nanotubes 37 μm in the length and ~110 nm in the diameter was reported to receive a moderate efficiency of ~5.0%.

Spherical oxide aggregate nanostructures

ZnO aggregates

Aggregates are a type of 3D nanostructure with spherical assembling of nanocrystallites or other nanomaterials. The use of aggregates in DSCs is based on a consideration that, while size in the range of submicron meters, i.e., compara-

ble to the wavelengths of the visible light, the aggregates may generate an effective light scattering and, thus, significantly increase the traveling distance of the light within the photoelectrode film. This leads to an increased opportunity for the photons to interact with the dye molecules adsorbed on nanocrystallites, and as such, enhances the light harvesting efficiency of photoelectrode.

Light scattering is already a well-known approach used in the conventional DSCs for boosting the optical absorption of photoelectrode. To generate light scattering, one of traditional methods is to mix nanoparticle with ~400 nm large particles that serve as light scatterers. Another way, which is different from the mixture structure, is to place the large particles at the top of the nanoparticle film so as to form a light scattering layer [90]. Both these methods have been proved to be effective in introducing light scattering and, accordingly, enhancing the optical absorption of photoelectrode in DSCs. However, an obvious drawback of the use of large particles as light scatterers is that these large particles unavoidably cause either a loss of surface area to the photoelectrode film (in the case of a mixture structure) or an increase in the film thickness (in the case of double-layer structure). In comparison with large particles, to act as light scatterers the aggregates take an obvious advantage in structure, i.e., the aggregates possess a highly porous structure by reason of consisting of nanosized crystallites. That means, while forming a photoelectrode film, the aggregates would not only work as light scatterers, but also be able to undertake dye loading and make contribution to optical absorption. In other words, a use of aggregates would not cause any significant sacrifice of the surface area of photoelectrode film.

The rationality of scenario mentioned above has been well evidenced by an example concerning ZnO aggregates. The ZnO aggregates were synthesized by hydrolysis of zinc salt in a polyol medium [69]. Under SEM observation, the as-prepared aggregates were shown a structure of spherical assembling of nanocrystallites and diameter size in submicrometer region (Fig. 13a and b). X-ray diffraction (XRD) characterization was employed to reveal an average crystallite size of ~15 nm. A BET measurement demonstrated a specific surface of approximately 80 m^2/g. A comparison of DSC performance between the films of aggregates and nanoparticles presented a significant difference in the conversion efficiencies, 2.4% and 5.4% for ZnO nanoparticles and aggregates, respectively (Fig. 13c), meaning an almost doubled enhancement in the overall conversion efficiency due to a use of the aggregate structure for photoelectrode [69]. This had been attributed to light scattering which was generated by the aggregates and could enhance the light harvesting efficiency of photoelectrode.

The enhancement mechanism with light scattering was verified by further studies which compared the efficiencies of photoelectrodes consisting of ZnO aggregates with different sizes and size distributions [178]. It was revealed that (1) the photoelectrodes with polydisperse aggregates yielded efficiencies generally higher than those obtained for photoelectrodes made of monodisperse ones, and (2) the aggregates with size closer to the light wavelength could result in efficiency enhancement more intensively. These results strengthened the rationality that enhanced solar-cell performance arose from light scattering owing to the aggregates.

In addition to light scattering, a less compact structure of the photoelectrode film consisting of ZnO aggregates is also thought to be a reason giving a high conversion efficiency by the aggregate solar cells. This is based on a consideration that ZnO is not stable in an acidic dye solution and the formation of a Zn^{2+}/dye complex on the surface of ZnO may seriously hinder the electron injection from dye molecules to the semiconductor [179]. In the case of film comprised of ZnO nanoparticles, the formation of complex on the film surface would block the pores and result in an uncompleted infiltration of dye molecules [180]. However, the situation is quite different in the case of aggregates. Due to the existence of large pores among the sub-micron sized aggregates, the dye penetration can be accomplished in a very short time (for example, 30 min) prior to the formation of complex layer [69,181].

Surface modification of ZnO aggregates with lithium ions [182] or ALD-deposited TiO_2 thin layer [183] may enhance the solar cell performance to some extent. The enhancement results from an improvement of the stability of ZnO for better dye adsorption. These treatments may else promote the chemical bonding between dye molecules and semiconductor, make electron injection more effective.

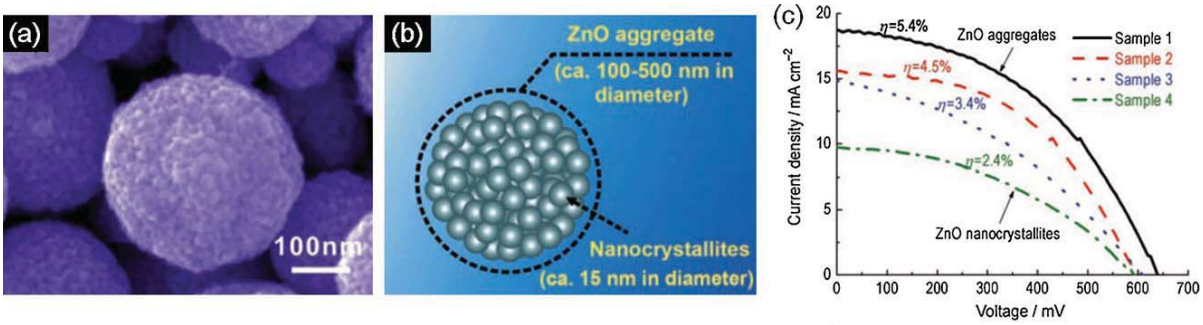

Figure 13 ZnO aggregates showing enhanced DSC performance in comparison with nanoparticles [69]: (a) SEM image and (b) schematic drawing of ZnO aggregates indicating a hierarchical structure of spherical assembling of nanocrystallites, and (c) photovoltaic curves of four ZnO samples, Sample 1: aggregates, Sample 2: aggregates with slight distortion of the spherical shape, Sample 3: parts of aggregates and nanocrystallites, Sample 4: nanocrystallites.

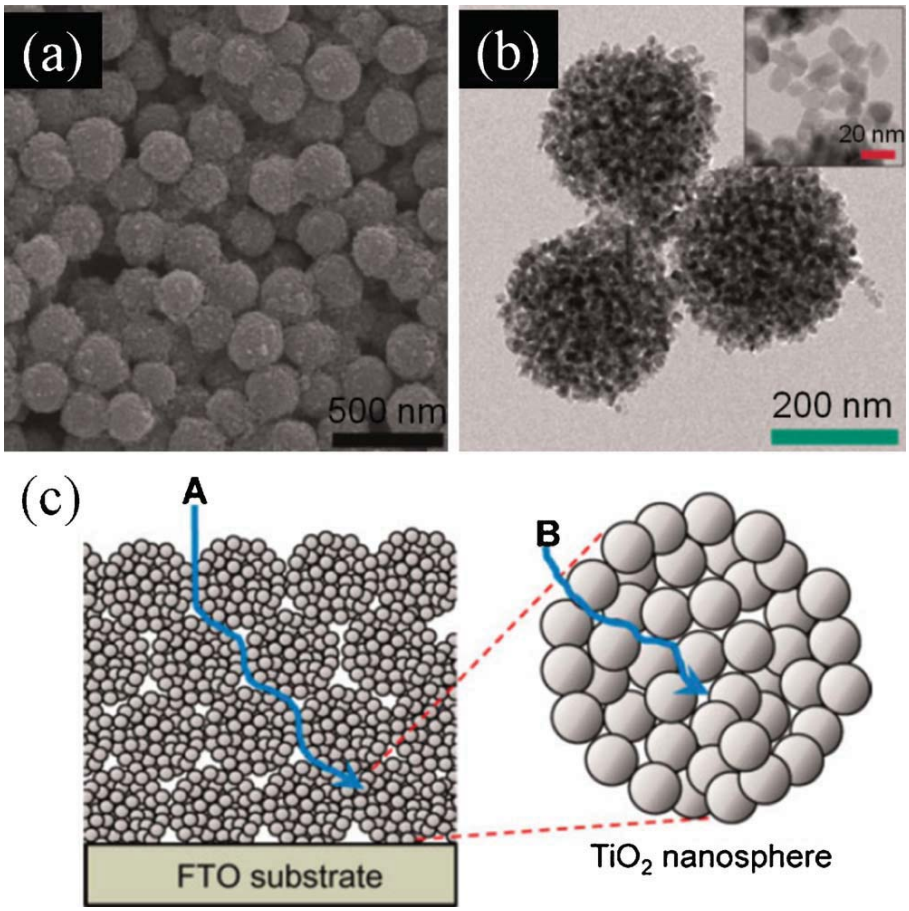

Figure 14 Nanoporous TiO_2 spheres for application in DSCs [184]. (a) SEM and (b) TEM images of nanoporous TiO_2 spheres, and (c) schematic diagram showing the electrolyte diffusion through the external (A) and internal (B) pores in the film made of nanoporous TiO_2 spheres.

TiO_2 aggregates

TiO_2 aggregate structure was also developed recently for DSC application [184,185]. Kim et al. reported a two-step method for the synthesis of TiO_2 aggregates which first fabricated TiO_2 spheres via a controlled hydrolysis and then etched the spheres under a hydrothermal condition; the latter step enables the spheres to convert to be of crystallized structure with high porosity, forming the so-called nanoporous TiO_2 spheres, which are approximately 250 nm in diameter and consist of nanocrystallites with a size of about 12 nm (Fig. 14a and b) [184]. These aggregates demonstrated a very high surface area, ~117.9 m^2/g, which was 1.7 times that of nanoparticles. Applying these aggregates to DSCs yielded an efficiency as high as 10.5%.

Rather than a light scattering mechanism that is described in the section of ZnO aggregates, the high efficiency was explained by reason that the film comprised of TiO_2 aggregates could provide a ''highway'' for electrolyte diffusion in view of the existence of 150—300-nm-sized pores (denoted as ''A'' in Fig. 14c) originating from the interstitial voids among the 250-nm-sized spheres. Such a quick diffusion of electrolyte throughout the film facilitated a further diffusion of I_3^- ion into the internal pores (denoted as ''B'' in Fig. 14c) owing to a short diffusion distance just from the outside of spheres to the interior.

Conclusions and outlook

DSCs have kept their efficiency record at 10—11% for many years, which are however far lower than the theoretically predicted one, ~20% [33,48]. In principle, there are three potential ways that may achieve a breakthrough in the conversion efficiency of DSCs [163]. One way based on a consideration of boosting the light harvesting efficiency of photoelectrode is to develop new photosensitizers with higher molar extinction coefficient and broader spectral response than the existing dyes. This point has been well manifested to be both direct and effective by the history and development of DSCs over the past decades. Of course, the chemists have never stopping seeking for more powerful photosensitizers including organic dyes and other types, for example, quantum dots [186—188], and energy relay dyes [189]. The second way is to possibly improve the open-circuit voltage of DSCs. Open-circuit voltage is known to be determined by the energy difference between the quasi-Fermi

levels of the electrons in semiconductor and the redox couple in electrolyte. It therefore requires finding electrolytes with a redox couple more closely matched to the energy of the oxidized dye to, as such, increase the open-circuit voltage. It was estimated that a 300 mV increase in the open-circuit voltage would mean a 35% improvement in the device efficiency, i.e., reaching ~14% [163]. Some recent studies focusing on ionic liquid electrolytes show great promises in increasing the open-circuit voltage [190—193]. The third way is to reduce the energy loss in the solar cell caused by, for example, charge recombination, electron trapping, optical reflection, and so on. In this regard, nanotechnology with capability of tailoring materials for defined purpose may create abundant nanostructures, and with these nanostructured materials it is possible to receive increased electron diffusion length, decreased back recombination, and physical effects such as photon localization, thus a decrease in the energy loss would likely lead to an improvement in the solar cell efficiency.

In considering nanostructured materials, the nanoparticles of TiO_2 are still predominant in achieving the maximum conversion efficiencies nowadays. This is attributed to a large surface area contributed by the nanoparticles and the exposed (1 0 1) planes of TiO_2 nanoparticles which may yield ideal chemisorption with those existing dyes. A further decrease in the nanoparticle size can indeed lead to an increase in the surface area of photoelectrode film. However, due to a simultaneously happened decrease in the pore size and increase in the defect sites and grain boundaries, use of smaller nanoparticles would eventually lower the solar cell performance. This is also the reason that optimum size for the TiO_2 nanoparticles has been reported to be in a range of 12—20 nm [58,194,195]. Surface modification or doping of TiO_2 have also shown complication and lack of reproducibility, as partially shown in the section of core—shell nanostructures mentioned above [196]. Therefore, it seems that there is only limited room for improving the solar cell performance by optimizing the photoelectrode film made of nanoparticles.

As for the one-dimensional nanostructures, although they have announced an extremely long electron diffusion length, up to 100 μm [137], currently most of the DSCs made of one-dimensional nanostructures show efficiencies much lower than those obtained for the TiO_2 nanoparticles. This is because of the limit in the surface area of the one-dimensional nanostructures. To increase the surface area basically relies on an increase in the length of the one-dimensional nanostructures. However, this is facing a difficulty in the fabrication technique, for example, how to avoid a bottom attachment for the nanowire or nanotube array while their length is over several tens micron meters. On the other hand, the fabrication of ultra-long nanowires or nanotubes would become more difficult in the case of transparent conductive substrate.

As an outlook, the paper would like to put stress on the aggregate structure, which possesses surface area comparable to that of nanoparticles and, meanwhile, shows capability of generating light scattering. It is understood that light scattering is effective in extending the traveling distance of incident light within photoelectrode film. This may significantly enhances the light harvesting efficiency of photoelectrode. It is therefore rational that, with a use of aggregates, the photoelectrode film would allow to be thinner than the conventional ones. The importance of this point is that a thinner photoelectron film means a shortening of the distance for the photogenerated electrons to travel from the site occurring electron injection to the FTO film of collecting electrode. As such, the charge recombination rate in a DSC can be significantly lowered and, therefore, one can expect a breakthrough of the dye-sensitized solar cell efficiency. However, there is a challenge to the synthesis of TiO_2 aggregates with suitable size, porosity, and surface chemistry.

Acknowledgements

This work is supported by the U.S. Department of Energy, Office of Basic Energy Sciences, Division of Materials and Engineering under Award No. DE-FG02-07ER46467 (Q.F.Z.), National Science Foundation (DMR 1035196), the Air Force Office of Scientific Research (AFOSR-MURI, FA9550-06-1-0326) (K.S.P.), the University of Washington TGIF grant, the Washington Research Foundation, and the Intel Corporation.

References

[1] G. Cao, Nanostructures & Nanomaterials: Synthesis, Properties & Applications, Imperial College Pr, 2004.
[2] E. Wolf, Nanophysics and Nanotechnology: An Introduction to Modern Concepts in Nanoscience, Vch Verlagsgesellschaft Mbh, 2006.
[3] Y.N. Xia, P.D. Yang, Y.G. Sun, Y.Y. Wu, B. Mayers, B. Gates, Y.D. Yin, F. Kim, Y.Q. Yan, Adv. Mater. 15 (2003) 353—389.
[4] M. Ratner, D. Ratner, Nanotechnology: A Gentle Introduction to the Next Big Idea, Prentice Hall Press Upper Saddle River, NJ, USA, 2002.
[5] D. Feldheim, C. Foss, Metal Nanoparticles: Synthesis, Characterization and Applications, CRC, 2002.
[6] T. Sugimoto, Fine Particles: Synthesis, Characterization and Mechanisms of Growth, CRC, 2000.
[7] M. Grätzel, J. Sol-Gel Sci. Technol 22 (2001) 7—13.
[8] C.M. Lieber, Z.L. Wang, MRS Bull. 32 (2007) 99—108.
[9] K. Sattler, Handbook of Nanophysics: Nanotubes and Nanowires, CRC, 2011.
[10] Z. Wang, Nanowires and Nanobelts: Materials Properties and Devices: Volume 2: Nanowires and Nanobelts of Functional Materials, Springer-Verlag, 2005.
[11] R. Saito, G. Dresselhaus, M. Dresselhaus, Physical Properties of Carbon Nanotubes, Imperial College Press, London, 1999.
[12] R.H. Baughman, A.A. Zakhidov, W.A. de Heer, Science 297 (2002) 787—792.
[13] Z.W. Pan, Z.R. Dai, Z.L. Wang, Science 291 (2001) 1947—1949.
[14] Z. Wang, J. Nanosci. Nanotechnol. 8 (2008) 27—55.
[15] D. Jezequel, J. Guenot, N. Jouini, F. Fievet, Trans. Tech. Publ. (1994) 339—342.
[16] Y Zhou, M. Antonietti, J. Am. Chem. Soc. 125 (2003) 14960—14961.
[17] M. Chamarro, C. Gourdon, P. Lavallard, O. Lublinskaya, A.I. Ekimov, Phys. Rev. B 53 (1996) 1336—1342.
[18] Y. Gu, I. Kuskovsky, M. Yin, S. O'Brien, G. Neumark, Appl. Phys. Lett. 85 (2004) 3833.
[19] B. Delley, E. Steigmeier, Phys. Rev. B 47 (1993) 1397—1400.
[20] J. Joannopoulos, J. Winn, Photonic Crystals: Molding The Flow of Light, Princeton Univ Pr, 2008.
[21] E. Kumacheva, R.K. Golding, M. Allard, E.H. Sargent, Adv. Mater. 14 (2002) 221—224.

[22] M. Rajalakshmi, A.K. Arora, B.S. Bendre, S. Mahamuni, J. Appl. Phys. 87 (2000) 2445—2448.
[23] A. Yamilov, X. Wu, X. Liu, R.P.H. Chang, H. Cao, Phys. Rev. Lett. 96 (2006) 083905.
[24] S.S. Fan, M.G. Chapline, N.R. Franklin, T.W. Tombler, A.M. Cassell, H.J. Dai, Science 283 (1999) 512—514.
[25] M. Grätzel, Nature 414 (2001) 338—344.
[26] Q.F. Zhang, C.S. Dandeneau, X.Y. Zhou, G.Z. Cao, Adv. Mater. 21 (2009) 4087—4108.
[27] M. Grundmann, Nano-optoelectronics: Concepts, Physics and Devices, Springer-Verlag, 2002.
[28] F. Patolsky, C. Lieber, Mater. Today 8 (2005) 20—28.
[29] M. Grätzel, Inorg. Chem. 44 (2005) 6841—6851.
[30] J. Perlin, National Renewable Energy Lab., Golden, CO., US, 2004.
[31] A. Shah, H. Schade, M. Vanecek, J. Meier, E. Vallat-Sauvain, N. Wyrsch, U. Kroll, C. Droz, J. Bailat, Progr. Photovoltaics: Res. Appl. 12 (2004) 113—142.
[32] K. Chopra, P. Paulson, V. Dutta, Progr. Photovoltaics: Res. Appl. 12 (2004) 69—92.
[33] M. Grätzel, J. Photochem. Photobiol. C: Photochem. Rev. 4 (2003) 145—153.
[34] A. Hagfeldt, M. Grätzel, Acc. Chem. Res. 33 (2000) 269—277.
[35] H. Hoppe, N. Sariciftci, J. Mater. Res. 19 (2004) 1924—1945.
[36] D. Wohrle, D. Meissner, Adv. Mater. 3 (1991) 129—138.
[37] M. Green, K. Emery, Y. Hishikawa, W. Warta, Progr. Photovoltaics: Res. Appl. 17 (2009) 320—326.
[38] M. Grätzel, Philos. Trans. Royal Soc. A: Math. Phys. Eng. Sci. 365 (2007) 993—1005.
[39] D. Kuang, J. Brillet, P. Chen, M. Takata, S. Uchida, H. Miura, K. Sumioka, S. Zakeeruddin, M. Gra tzel, ACS Nano 2 (2008) 1113—1116.
[40] F. Pichot, J. Pitts, B. Gregg, Langmuir 16 (2000) 5626—5630.
[41] S. Ito, N. Ha, G. Rothenberger, P. Liska, P. Comte, S. Zakeeruddin, P. Péchy, M. Nazeeruddin, M. Grätzel, Chem. Commun. 2006 (2006) 4004—4006.
[42] M. Späth, P. Sommeling, J. Van Roosmalen, H. Smit, N. Van Der Burg, D. Mahieu, N. Bakker, J. Kroon, Progr. Photovoltaics: Res. Appl. 11 (2003) 207—220.
[43] H. Chen, J. Hou, S. Zhang, Y. Liang, G. Yang, Y. Yang, L. Yu, Y. Wu, G. Li, Nature Photonics 3 (2009) 649—653.
[44] S.Y. Dai, J. Weng, Y.F. Sui, S.H. Chen, S.F. Xiao, Y. Huang, F.T. Kong, X. Pan, L.H. Hu, C.N. Zhang, K.J. Wang, Inorg. Chim. Acta 361 (2008) 786—791.
[45] Y. Chiba, A. Islam, Y. Watanabe, R. Komiya, N. Koide, L.Y. Han, Jpn. J. Appl. Phys. Part 2: Lett. Express Lett. 45 (2006) L638—L640.
[46] J.M. Kroon, N.J. Bakker, H.J.P. Smit, P. Liska, K.R. Thampi, P. Wang, S.M. Zakeeruddin, M. Grätzel, A. Hinsch, S. Hore, U. Wurfel, R. Sastrawan, J.R. Durrant, E. Palomares, H. Pettersson, T. Gruszecki, J. Walter, K. Skupien, G.E. Tulloch, Progr. Photovoltaics 15 (2007) 1—18.
[47] S. Ito, T. Murakami, P. Comte, P. Liska, C. Grätzel, M. Nazeeruddin, M. Grätzel, Thin Solid Films 516 (2008) 4613—4619.
[48] H.J. Snaith, Adv. Funct. Mater. 20 (2010) 13—19.
[49] A.J. Frank, N. Kopidakis, J. van de Lagemaat, Coord. Chem. Rev. 248 (2004) 1165—1179.
[50] A. Hauch, A. Georg, Electrochim. Acta 46 (2001) 3457—3466.
[51] N. Robertson, Angew. Chem.: Int. Edit. 45 (2006) 2338—2345.
[52] L. Schmidt-Mende, U. Bach, R. Humphry-Baker, T. Horiuchi, H. Miura, S. Ito, S. Uchida, M. Grätzel, Adv. Mater 17 (2005) 813—815.
[53] D.B. Kuang, S. Ito, B. Wenger, C. Klein, J.E. Moser, R. Humphry-Baker, S.M. Zakeeruddin, M. Grätzel, JACS 128 (2006) 4146—4154.
[54] D. Hagberg, J. Yum, H. Lee, F. De Angelis, T. Marinado, K. Karlsson, R. Humphry-Baker, L. Sun, A. Hagfeldt, M. Grätzel, JACS 130 (2008) 6259—6266.
[55] M. Nazeeruddin, P. Pechy, T. Renouard, S. Zakeeruddin, R. Humphry-Baker, P. Comte, P. Liska, E. Costa, V. Shklover, L. Spiccia, J. Am. Chem. Soc. 123 (2001) 1613—1624.
[56] C. Chen, S. Wu, C. Wu, J. Chen, K. Ho, Angew. Chem. 118 (2006) 5954—5957.
[57] C. Klein, M. Nazeeruddin, P. Liska, D. Di Censo, N. Hirata, E. Palomares, J. Durrant, M. Grätzel, Inorg. Chem. 44 (2005) 178—180.
[58] M.K. Nazeeruddin, A. Kay, I. Rodicio, R. Humphrybaker, E. Muller, P. Liska, N. Vlachopoulos, M. Grätzel, JACS 115 (1993) 6382—6390.
[59] M.K. Nazeeruddin, S.M. Zakeeruddin, R. Humphry-Baker, M. Jirousek, P. Liska, N. Vlachopoulos, V. Shklover, C.H. Fischer, M. Grätzel, Inorg. Chem. 38 (1999) 6298—6305.
[60] M.K. Nazeeruddin, P. Pechy, M. Grätzel, Chem. Commun. (1997) 1705—1706.
[61] P. Wang, C. Klein, R. Humphry-Baker, S. Zakeeruddin, M. Grätzel, J. Am. Chem. Soc. 127 (2005) 808—809.
[62] C.Y. Chen, M.K. Wang, J.Y. Li, N. Pootrakulchote, L. Alibabaei, C.H. Ngoc-le, J.D. Decoppet, J.H. Tsai, C. Grätzel, C.G. Wu, S.M. Zakeeruddin, M. Grätzel, ACS Nano 3 (2009) 3103—3109.
[63] F. Gao, Y. Wang, D. Shi, J. Zhang, M.K. Wang, X.Y. Jing, R. Humphry-Baker, P. Wang, S.M. Zakeeruddin, M. Grätzel, JACS 130 (2008) 10720—10728.
[64] B. Oregan, M. Grätzel, Nature 353 (1991) 737—740.
[65] D. Cahen, G. Hodes, M. Grätzel, J.F. Guillemoles, I. Riess, J. Phys. Chem. B 104 (2000) 2053—2059.
[66] M. Law, L.E. Greene, J.C. Johnson, R. Saykally, P.D. Yang, Nature Mater. 4 (2005) 455—459.
[67] S.Y. Huang, G. Schlichthorl, A.J. Nozik, M. Grätzel, A.J. Frank, J. Phys. Chem. B 101 (1997) 2576—2582.
[68] J. Van de Lagemaat, N. Park, A. Frank, J. Phys. Chem. B 104 (2000) 2044—2052.
[69] Q.F. Zhang, T.R. Chou, B. Russo, S.A. Jenekhe, G.Z. Cao, Angew. Chem.: Int. Edit. 47 (2008) 2402—2406.
[70] Q.F. Zhang, C.S. Dandeneau, K. Park, D.W. Liu, X.Y. Zhou, Y.H. Jeong, G.Z. Cao, J. Nanophotonics 4 (2010) 041540.
[71] M. Eisenberg, H. Silverman, Electrochim. Acta 5 (1961) 1—12.
[72] A. Nozik, Philos. Trans. Roy. Soc. Lond. Ser. A Math. Phys. Sci. 295 (1980) 453—470.
[73] R. Memming, Electrochim. Acta 25 (1980) 77—88.
[74] N. Alonso, M. Beley, P. Chartier, V. Ern, Rev. Phys. Appl. 16 (1981) 5—10.
[75] K. Rajeshwar, P. Singh, J. DuBow, Electrochim. Acta 23 (1978) 1117—1144.
[76] H.J. Danzmann, K. Hauffe, Ber Bunsen: Phys. Chem. Chem. Phys. 79 (1975) 438—453.
[77] S. Anderson, E.C. Constable, M.P. Dareedwards, J.B. Goodenough, A. Hamnett, K.R. Seddon, R.D. Wright, Nature 280 (1979) 571—573.
[78] A. Hamnett, M. Dare-Edwards, R. Wright, K. Seddon, J. Goodenough, J. Phys. Chem. 83 (1979) 3280—3290.
[79] B.W. Jing, M.H. Zhang, T. Shen, Chin. Sci. Bull. 42 (1997) 1937—1948.
[80] H.D. Abruna, A.Y. Teng, G.J. Samuels, T.J. Meyer, JACS 101 (1979) 6745—6746.
[81] J. Desilvestro, M. Grätzel, L. Kavan, J. Moser, J. Augustynski, JACS 107 (1985) 2988—2990.
[82] R. Memming, Surf. Sci. 101 (1980) 551—563.
[83] W.D.K. Clark, N. Sutin, JACS 99 (1977) 4676—4682.
[84] M. Matsumura, Y. Nomura, H. Tsubomura, Bull. Chem. Soc. Jpn. 50 (1977) 2533—2537.
[85] M. Nazeeruddin, P. Liska, J. Moser, N. Vlachopoulos, M. Grätzel, Helv. Chim. Acta 73 (1990) 1788—1803.

[86] A. Polo, M. Itokazu, N. Murakami Iha, Coord. Chem. Rev. 248 (2004) 1343—1361.
[87] C.J. Barbe, F. Arendse, P. Comte, M. Jirousek, F. Lenzmann, V. Shklover, M. Grätzel, J. Am. Ceram. Soc. 80 (1997) 3157—3171.
[88] N.G. Park, J. van de Lagemaat, A.J. Frank, J. Phys. Chem. B 104 (2000) 8989—8994.
[89] M. Grätzel, Progr. Photovoltaics 8 (2000) 171—185.
[90] F.T. Kong, S.Y. Dai, K.J. Wang, Adv. OptoElectron. 2007 (2007) 75384.
[91] M. Nazeeruddin, C. Klein, P. Liska, M. Grätzel, Coord. Chem. Rev. 249 (2005) 1460—1467.
[92] M. Adachi, J. Jiu, S. Isoda, Curr. Nanosci. 3 (2007) 285—295.
[93] K. Keis, E. Magnusson, H. Lindstrom, S.E. Lindquist, A. Hagfeldt, Sol. Energy Mater. Sol. Cells 73 (2002) 51—58.
[94] K. Tennakone, G. Kumara, I.R.M. Kottegoda, V.P.S. Perera, Chem. Commun. (1999) 15—16.
[95] S. Chappel, A. Zaban, Sol. Energy Mater. Sol. Cells 71 (2002) 141—152.
[96] B.V. Bergeron, A. Marton, G. Oskam, G.J. Meyer, J. Phys. Chem. B 109 (2005) 937—943.
[97] K. Sayama, H. Sugihara, H. Arakawa, Chem. Mater. 10 (1998) 3825—3832.
[98] P. Guo, M.A. Aegerter, Thin Solid Films 351 (1999) 290—294.
[99] S. Burnside, J.E. Moser, K. Brooks, M. Grätzel, D. Cahen, J. Phys. Chem. B 103 (1999) 9328—9332.
[100] B. Tan, E. Toman, Y.G. Li, Y.Y. Wu, JACS 129 (2007) 4162—4163.
[101] P. Sommeling, B. O'Regan, R. Haswell, H. Smit, N. Bakker, J. Smits, J. Kroon, J. Van Roosmalen, J. Phys. Chem. B 110 (2006) 19191—19197.
[102] Y. Diamant, S.G. Chen, O. Melamed, A. Zaban, J. Phys. Chem. B 107 (2003) 1977—1981.
[103] Y. Diamant, S. Chappel, S.G. Chen, O. Melamed, A. Zaban, Coord. Chem. Rev. 248 (2004) 1271—1276.
[104] E. Palomares, J.N. Clifford, S.A. Haque, T. Lutz, J.R. Durrant, JACS 125 (2003) 475—482.
[105] S.G. Chen, S. Chappel, Y. Diamant, A. Zaban, Chem. Mater. 13 (2001) 4629—4634.
[106] A. Kay, M. Grätzel, Chem. Mater 14 (2002) 2930—2935.
[107] F. Fabregat-Santiago, J. Garcia-Canadas, E. Palomares, J.N. Clifford, S.A. Haque, J.R. Durrant, G. Garcia-Belmonte, J. Bisquert, J. Appl. Phys. 96 (2004) 6903—6907.
[108] S. Chappel, S.G. Chen, A. Zaban, Langmuir 18 (2002) 3336—3342.
[109] N.G. Park, M.G. Kang, K.M. Kim, K.S. Ryu, S.H. Chang, D.K. Kim, J. van de Lagemaat, K.D. Benkstein, A.J. Frank, Langmuir 20 (2004) 4246—4253.
[110] J. Nelson, R.E. Chandler, Coord. Chem. Rev. 248 (2004) 1181—1194.
[111] J. van de Lagemaat, N.G. Park, A.J. Frank, J. Phys. Chem. B 104 (2000) 2044—2052.
[112] L. Peter, Phys. Chem. Chem. Phys. 9 (2007) 2630—2642.
[113] L. Dloczik, O. Ileperuma, I. Lauermann, L.M. Peter, E.A. Ponomarev, G. Redmond, N.J. Shaw, I. Uhlendorf, J. Phys. Chem. B 101 (1997) 10281—10289.
[114] A.C. Fisher, L.M. Peter, E.A. Ponomarev, A.B. Walker, K.G.U. Wijayantha, J. Phys. Chem. B 104 (2000) 949—958.
[115] L. Forro, O. Chauvet, D. Emin, L. Zuppiroli, H. Berger, F. Levy, J. Appl. Phys. 75 (1994) 633—635.
[116] X.J. Feng, K. Shankar, O.K. Varghese, M. Paulose, T.J. Latempa, C.A. Grimes, Nano Lett. 8 (2008) 3781—3786.
[117] B. Liu, E.S. Aydil, JACS 131 (2009) 3985—3990.
[118] J.J. Qiu, X.M. Li, F.W. Zhuge, X.Y. Gan, X.D. Gao, W.Z. He, S.J. Park, H.K. Kim, Y.H. Hwang, Nanotechnology 21 (2010).
[119] H. Horiuchi, R. Katoh, K. Hara, M. Yanagida, S. Murata, H. Arakawa, M. Tachiya, J. Phys. Chem. B 107 (2003) 2570—2574.
[120] K. Keis, C. Bauer, G. Boschloo, A. Hagfeldt, K. Westermark, H. Rensmo, H. Siegbahn, J. Photochem. Photobiol. A: Chem. 148 (2002) 57—64.
[121] K. Fujihara, A. Kumar, R. Jose, S. Ramakrishna, S. Uchida, Nanotechnology 18 (2007) 365709.
[122] H. Kokubo, B. Ding, T. Naka, H. Tsuchihira, S. Shiratori, Nanotechnology 18 (2007) 165604.
[123] M. Song, D. Kim, K. Ihn, S. Jo, D. Kim, Nanotechnology 15 (2004) 1861—1865.
[124] P. Roy, D. Kim, K. Lee, E. Spiecker, P. Schmuki, Nanoscale 2 (2010) 45—59.
[125] K. Zhu, N. Neale, A. Miedaner, A. Frank, Nano Lett 7 (2007) 69—74.
[126] D. Gong, C.A. Grimes, O.K. Varghese, W.C. Hu, R.S. Singh, Z. Chen, E.C. Dickey, J. Mater. Res. 16 (2001) 3331—3334.
[127] G.K. Mor, O.K. Varghese, M. Paulose, K. Shankar, C.A. Grimes, Sol. Energy Mater. Sol. Cells 90 (2006) 2011—2075.
[128] A. Ghicov, P. Schmuki, Chem. Commun. (2009) 2791—2808.
[129] M. Paulose, K. Shankar, S. Yoriya, H.E. Prakasam, O.K. Varghese, G.K. Mor, T.A. Latempa, A. Fitzgerald, C.A. Grimes, J. Phys. Chem. B 110 (2006) 16179—16184.
[130] K. Shankar, G.K. Mor, H.E. Prakasam, S. Yoriya, M. Paulose, O.K. Varghese, C.A. Grimes, Nanotechnology 18 (2007).
[131] H.E. Prakasam, K. Shankar, M. Paulose, O.K. Varghese, C.A. Grimes, J. Phys. Chem. C 111 (2007) 7235—7241.
[132] C.M. Ruan, M. Paulose, O.K. Varghese, G.K. Mor, C.A. Grimes, J. Phys. Chem. B 109 (2005) 15754—15759.
[133] M. Paulose, H.E. Prakasam, O.K. Varghese, L. Peng, K.C. Popat, G.K. Mor, T.A. Desai, C.A. Grimes, J. Phys. Chem. C 111 (2007) 14992—14997.
[134] T. Stergiopoulos, A. Ghicov, V. Likodimos, D.S. Tsoukleris, J. Kunze, P. Schmuki, P. Falaras, Nanotechnology 19 (2008) 235602.
[135] J.M. Macak, H. Tsuchiya, A. Ghicov, P. Schmuki, Electrochem. Commun. 7 (2005) 1133—1137.
[136] M. Paulose, K. Shankar, O.K. Varghese, G.K. Mor, B. Hardin, C.A. Grimes, Nanotechnology 17 (2006) 1446—1448.
[137] J.R. Jennings, A. Ghicov, L.M. Peter, P. Schmuki, A.B. Walker, JACS 130 (2008) 13364—13372.
[138] A. Ghicov, S.P. Albu, R. Hahn, D. Kim, T. Stergiopoulos, J. Kunze, C.A. Schiller, P. Falaras, P. Schmuki, Chem.: Asian J. 4 (2009) 520—525.
[139] G.K. Mor, K. Shankar, M. Paulose, O.K. Varghese, C.A. Grimes, Nano Lett 6 (2006) 215—218.
[140] T. Stergiopoulos, A. Valota, V. Likodimos, T. Speliotis, D. Niarchos, P. Skeldon, G.E. Thompson, P. Falaras, Nanotechnology 20 (2009).
[141] C.A. Grimes, J. Mater. Chem. 17 (2007) 1451—1457.
[142] G.K. Mor, O.K. Varghese, M. Paulose, C.A. Grimes, Adv. Funct. Mater. 15 (2005) 1291—1296.
[143] J.H. Park, T.W. Lee, M.G. Kang, Chem. Commun. (2008) 2867—2869.
[144] K. Zhu, T.B. Vinzant, N.R. Neale, A.J. Frank, Nano Lett. 7 (2007) 3739—3746.
[145] D. Kim, A. Ghicov, P. Schmuki, Electrochem. Commun. 10 (2008) 1835—1838.
[146] P. Roy, S.P. Albu, P. Schmuki, Electrochem. Commun. 12 (2010) 949—951.
[147] D. Kim, A. Ghicov, S.P. Albu, P. Schmuki, JACS 130 (2008) 16454—16455.
[148] J.B. Han, F.R. Fan, C. Xu, S.S. Lin, M. Wei, X. Duan, Z.L. Wang, Nanotechnology 21 (2010) 405203.
[149] A.B.F. Martinson, T.W. Hamann, M.J. Pellin, J.T. Hupp, Chem.: Eur. J. 14 (2008) 4458—4467.
[150] A.B.F. Martinson, J.W. Elam, J.T. Hupp, M.J. Pellin, Nano Lett 7 (2007) 2183—2187.

[151] A.B.F. Martinson, M.S. Goes, F. Fabregat-Santiago, J. Bisquert, M.J. Pellin, J.T. Hupp, J. Phys. Chem. A 113 (2009) 4015—4021.
[152] C.H. Ku, J.J. Wu, Nanotechnology 18 (2007) 505706.
[153] Y.Q. Wang, Y.M. Sun, K. Li, Mater. Lett. 63 (2009) 1102—1104.
[154] X.Y. Gan, X.M. Li, X.D. Gao, F.W. Zhuge, W.D. Yu, Thin Solid Films 518 (2010) 4809—4812.
[155] C.H. Ku, J.J. Wu, Appl. Phys. Lett. 91 (2007) 093117.
[156] S. Yodyingyong, Q.F. Zhang, K. Park, C.S. Dandeneau, X.Y. Zhou, D. Triampo, G.Z. Cao, Appl. Phys. Lett. 96 (2010) 073115.
[157] Y. Alivov, Z.Y. Fan, Appl. Phys. Lett. 95 (2009) 063504.
[158] P. Roy, D. Kim, I. Paramasivam, P. Schmuki, Electrochem. Commun. 11 (2009) 1001—1004.
[159] D. Kim, P. Roy, K. Lee, P. Schmuki, Electrochem. Commun. 12 (2010) 574—578.
[160] S. Ngamsinlapasathian, S. Sakulkhaemaruethai, S. Pavasupree, A. Kitiyanan, T. Sreethawong, Y. Suzuki, S. Yoshikawa, J. Photochem. Photobiol. A: Chem. 164 (2004) 145—151.
[161] B. Tan, Y.Y. Wu, J. Phys. Chem. B 110 (2006) 15932—15938.
[162] K. Asagoe, Y. Suzuki, S. Ngamsinlapasathian, S. Yoshikawa, TiO_2-anatase nanowire dispersed composite electrode for dye-sensitized solar cells, in: International Conference on Nanoscience and Technology (ICN&T 2006), IOP Publishing, 2007, pp. 1112—1116.
[163] M. Law, L.E. Greene, A. Radenovic, T. Kuykendall, J. Liphardt, P.D. Yang, J. Phys. Chem. B 110 (2006) 22652—22663.
[164] S. Gubbala, V. Chakrapani, V. Kumar, M.K. Sunkara, Adv. Funct. Mater. 18 (2008) 2411—2418.
[165] E. Joanni, R. Savu, M.D. Goes, P.R. Bueno, J.N. de Freitas, A.F. Nogueira, E. Longo, J.A. Varela, Scripta Mater. 57 (2007) 277—280.
[166] T.Y. Lee, P.S. Alegaonkar, J.B. Yoo, Thin Solid Films 515 (2007) 5131—5135.
[167] K. Uzaki, T. Nishimura, J. Usagawa, S. Hayase, M. Kono, Y. Yamaguchi, J. Solar Energy Eng. — Trans. ASME 132 (2010) 021204.
[168] G.Y. Chen, M.W. Lee, G.J. Wang, Int. J. Photoenergy (2010) 585621.
[169] W. Chen, H.F. Zhang, I.M. Hsing, S.H. Yang, Electrochem. Commun. 11 (2009) 1057—1060.
[170] Y.F. Hsu, Y.Y. Xi, C.T. Yip, A.B. Djurisic, W.K. Chan, J. Appl. Phys. 103 (2008) 083114.
[171] J.B. Baxter, A.M. Walker, K. van Ommering, E.S. Aydil, Nanotechnology 17 (2006) S304—S312.
[172] C.Y. Jiang, X.W. Sun, G.Q. Lo, D.L. Kwong, J.X. Wang, Appl. Phys. Lett. 90 (2007) 263501.
[173] F. Sauvage, F. Di Fonzo, A.L. Bassi, C.S. Casari, V. Russo, G. Divitini, C. Ducati, C.E. Bottani, P. Comte, M. Graetzel, Nano Lett. 10 (2010) 2562—2567.
[174] H.M. Cheng, W.H. Chiu, C.H. Lee, S.Y. Tsai, W.F. Hsieh, J. Phys. Chem. C 112 (2008) 16359—16364.
[175] J.B. Baxter, E.S. Aydil, Sol. Energy Mater. Sol. Cells 90 (2006) 607—622.
[176] C. Rustomji, C. Frandsen, S. Jin, M. Tauber, J. Phys. Chem. B (2010) (Published online June 7, 2010).
[177] J.B. Baxter, E.S. Aydil, Appl. Phys. Lett. 86 (2005) 053114.
[178] Q.F. Zhang, T.P. Chou, B. Russo, S.A. Jenekhe, G. Cao, Adv. Funct. Mater. 18 (2008) 1654—1660.
[179] M. Quintana, T. Edvinsson, A. Hagfeldt, G. Boschloo, J. Phys. Chem. C 111 (2007) 1035—1041.
[180] T.P. Chou, Q.F. Zhang, G.Z. Cao, J. Phys. Chem. C 111 (2007) 18804—18811.
[181] T.P. Chou, Q.F. Zhang, G.E. Fryxell, G.Z. Cao, Adv. Mater. 19 (2007) 2588—2592.
[182] Q.F. Zhang, C.S. Dandeneau, S. Candelaria, D.W. Liu, B.B. Garcia, X.Y. Zhou, Y.H. Jeong, G.Z. Cao, Chem. Mater. 22 (2010) 2427—2433.
[183] K. Park, Q.F. Zhang, B.B. Garcia, X.Y. Zhou, Y.H. Jeong, G.Z. Cao, Adv. Mater. 22 (2010) 2329—2332.
[184] Y.J. Kim, M.H. Lee, H.J. Kim, G. Lim, Y.S. Choi, N.G. Park, K. Kim, W.I. Lee, Adv. Mater. 21 (2009) 3668—3673.
[185] H.J. Koo, Y.J. Kim, Y.H. Lee, W.I. Lee, K. Kim, N.G. Park, Adv. Mater. 20 (2008) 195—199.
[186] P.V. Kamat, J. Phys. Chem. C 112 (2008) 18737—18753.
[187] R.D. Schaller, V.M. Agranovich, V.I. Klimov, Nature Phys. 1 (2005) 189—194.
[188] I. Robel, V. Subramanian, M. Kuno, P.V. Kamat, JACS 128 (2006) 2385—2393.
[189] B.E. Hardin, E.T. Hoke, P.B. Armstrong, J.H. Yum, P. Comte, T. Torres, J.M.J. Frechet, M.K. Nazeeruddin, M. Grätzel, M.D. McGehee, Nature Photonics 3 (2009) 406—411.
[190] D. Shi, N. Pootrakulchote, R.Z. Li, J. Guo, Y. Wang, S.M. Zakeeruddin, M. Grätzel, P. Wang, J. Phys. Chem. C 112 (2008) 17046—17050.
[191] P. Wang, S.M. Zakeeruddin, I. Exnar, M. Grätzel, Chem. Commun. (2002) 2972—2973.
[192] P. Wang, S.M. Zakeeruddin, P. Comte, I. Exnar, M. Grätzel, JACS 125 (2003) 1166—1167.
[193] P. Wang, S.M. Zakeeruddin, J.E. Moser, M. Grätzel, J. Phys. Chem. B 107 (2003) 13280—13285.
[194] S. Nakade, Y. Saito, W. Kubo, T. Kitamura, Y. Wada, S. Yanagida, J. Phys. Chem. B 107 (2003) 8607—8611.
[195] M. Grätzel, J. Photochem. Photobiol. A: Chem. 164 (2004) 3—14.
[196] K. Ko, Y. Lee, Y. Jung, J Colloid Interface Sci. 283 (2005) 482—487.

Qifeng Zhang, Ph.D., is currently working at University of Washington as a Research Assistant Professor. His research interests involve engineering applications of nanostructured materials in electronic devices including the solar cells, UV light-emitting diodes (LEDs), field-effect transistors (FETs), and gas sensors.

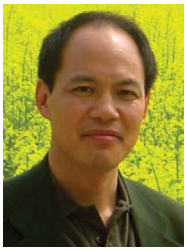

Guozhong Cao, Ph.D., is Boeing-Steiner Professor of Materials Science and Engineering and Adjunct Professor of Chemical and Mechanical Engineering at the University of Washington. He has published over 250 refereed papers, and authored and edited 5 books including ''Nanostructures and Nanomaterials''. His current research is focused mainly on nanomaterials for energy conversion and storage including solar cells, lithium-ion batteries, supercapacitors, and hydrogen storage materials.